Chapter - 3

Reduced Ground Plane Effects in Hexagonal Planar Antenna

3.1. Introduction

After a suitable comparison in chapter 2, hexagonal antenna is chosen for further exploration and investigation as a point of research work presented in this thesis and chapter. Narrow impedance bandwidth and dual resonance are characteristics of the probe fed quarter wave hexagonal patch antenna as it can be concluded from chapter 2. In this chapter a ground plane reduction is used as a technique to match the impedance, to suppress adjacent resonance and to achieve low cross polarization level at least in antenna boresight.

The effect of ground plane size reduction was theoretically investigated by Tong et al. using CST Microwave Studio (CST MWS) to model different cases, and a minimum ground plane size was recommended in (Tong 2011). The ground plane perturbation and enhancement of bandwidth by reducing the area of the ground by etching slots in it, was presented earlier in (Islam 2015). A design strategy was developed for coplanar antenna with a strip-ring-shaped reduced ground plane surrounding a circular patch for UWB applications. The measured return loss was less than −15 dB within 1.8 GHz to 13.5 GHz band, and its efficiency was 93% (Marynowski 2009). An antenna was designed to study the reduced-ground plane effects by cutting a notch from the radiator to concentrate the electric current on the radiator at lower operating frequencies for mobile devices (Chen 2007).

Noghanian et al. investigated circular patch antenna to observe effect of change in ground plane size and shape on radiation patterns of the antenna (Noghanian 1998). A monopole-like radiation pattern is achieved by reducing ground plane of rectangular patch antenna (John

2008). The suppression of undesired radiation and isolation between co and cross polarization has been achieved using defected ground structure (Kumar 2017).

Octagonal shaped antenna with the reduced ground plane has been fabricated by Norra et al. (Norra 2007) which has an operating bandwidth of 230 MHz. The dumbbell shaped defected ground structure (DGS) cell effect on the dimension of MSA was presented by Arya et al. and the cavity backed model was utilized to increase the efficiency of the antenna (Arya 2008). The H-shaped patch antenna modified with slots and ground plane have been designed and analyzed by Razali et al. for WIMAX application (2.45 GHz) (Razali 2015). The ground perturbation and reducing the area of the ground by etching slots to enhance the bandwidth has been presented earlier (Islam 2015).

Hexagonal structure and its configurations such as regular hexagon, half hexagon, shorted half hexagon and quarter hexagon were proposed and investigated in detail (Kumar 2003) (Ray 2013) (Bilotti 2010). Hexagonal antennas excite higher modes and exhibit wide-band behavior at high frequencies when the probe is directly fed to the vertex of hexagon (Joshi 2015a) (Joshi 2015b). Additional resonances are observed due to impedance mismatch in probe-fed hexagonal patch antenna (Joshi 2016b). It is essential to identify a technique to match the impedance in case of a thin substrate (thickness is less than $\lambda/10$) when directly fed through probe to obtain matched impedance. Ground plane reduction technique can be used to achieve impedance matching as was demonstrated for the clamshell mobile phone (Lee 2009). The effect of the ground plane is minimized when monopole antennas are designed for UWB applications (Ellis 2015) (Chen 2007). WSN nodes radiating through antennas with truncated ground plane were developed in order to optimize the size and the bandwidth constraint (Kakoyiannis 2009). Ground plane reduction technique is also used to achieve ultra wideband in a coplanar antenna (Marynowski 2009). The effect of dimensions of ground plane on radiation patterns of the antenna had been investigated by Noghanian et al

(Noghanian 1998). Truncation of the ground plane has an influence on gain as well as on the impedance bandwidth of an antenna as revealed by the parametric studies (Ansal 2015). The effect of size of a ground plane on performance of a probe-fed antenna had been studied and analyzed (Jha 2013). A potential solution to overcome the issue of impedance mismatch is reduced ground technique. The impedance matching using defected ground structure has been achieved in (Kumar 2017). Tong et al. theoretically investigated the effect of ground plane size reduction and recommended the minimum ground plane size (Tong 2011). The reduced ground technique is utilized to match the impedance of the patch with the probe in vertex fed hexagonal patch antenna.

In this chapter, an impedance matched vertex-fed hexagonal antenna with truncated ground plane is proposed and analyzed experimentally. This chapter also describes structure of proposed antennas while demonstrating the effect of ground plane reduction in C-Band. Besides an impedance match, reduction of ground plane suppresses additional resonances if any. This chapter proposes a method to improve impedance matching, lower cross polarizations levels and suppression of adjacent resonances if any in directly vertex-fed hexagonal antenna by reducing the ground plane.

Section 3.2 presents the probe fed slotted hexagon antenna with reduced ground for WLAN but with spurious radiation. In section 3.3 the reduced ground plane dimensions are optimized to suppress the spurious radiation of the probe fed hexagon antenna. In section 3.4 the reduced ground antenna is scaled down to radiate in X-band. Section 3.5 shows that low cross polarization can be achieved when ground plane dimension of probe fed hexagon antenna is optimized.

It is significant to note that the techniques described in this chapter have been presented for probe fed hexagonal antenna. Since wide bandwidth can be achieved using hexagon due to dual resonance property of hexagon geometry.

3.2. Vertex Fed Hexagonal C-Band Antenna

The compact regular hexagonal shaped patch antenna with hexagonal slot and reduced ground plane is designed and optimized at 5.5 GHz within C-band as shown in Figure 3.1.

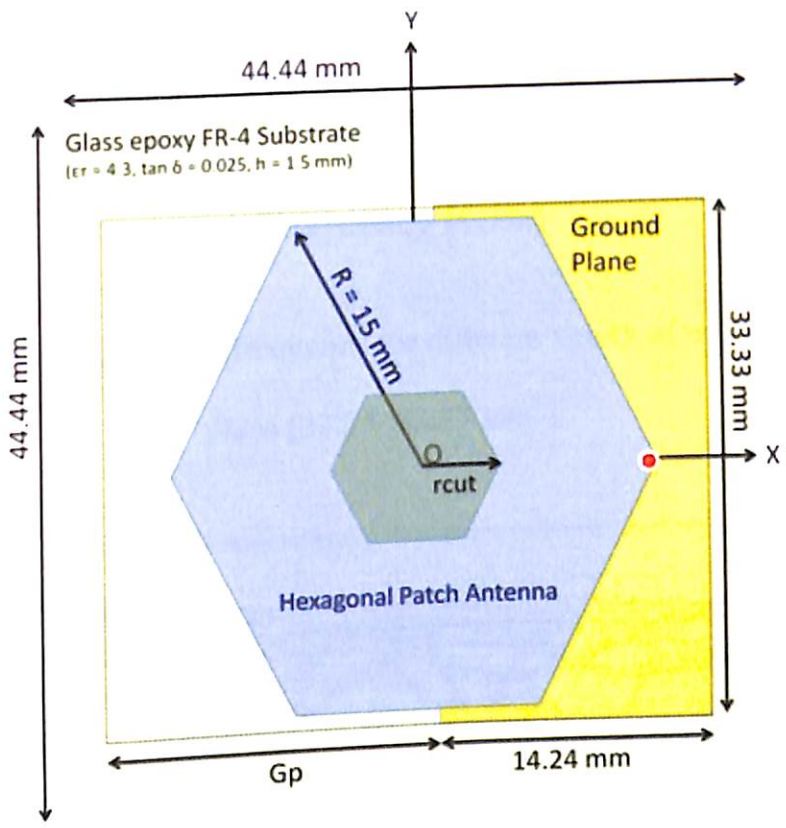

Figure 3.1. Schematic of the hexagonal shaped patch antenna with hexagonal slot and reduced ground.

The antenna uses a glass epoxy FR-4 substrate (ε_r = 4.3, tan δ = 0.025) of thickness (h = 1.5 mm) with dimension of 44.44 × 44.44 mm^2. The ground plane has the dimension of 14.24 × 33.33 mm^2. The hexagonal shaped patch size is around 0.5500 λ_o × 0.4763 λ_o in terms of the wavelength of the resonant frequency with a hexagonal slot with circumradius (*rcut*) of 2.5 mm. The SMA connector is placed near the vertex at a distance of 14 mm from center of patch using the analysis suggested in (Joshi 2015d). The SMA connector has the pin radius of 0.62 mm, dielectric (Teflon) radius of 2.076 mm and outer conductor of 2.565 mm with a height of 10 mm.

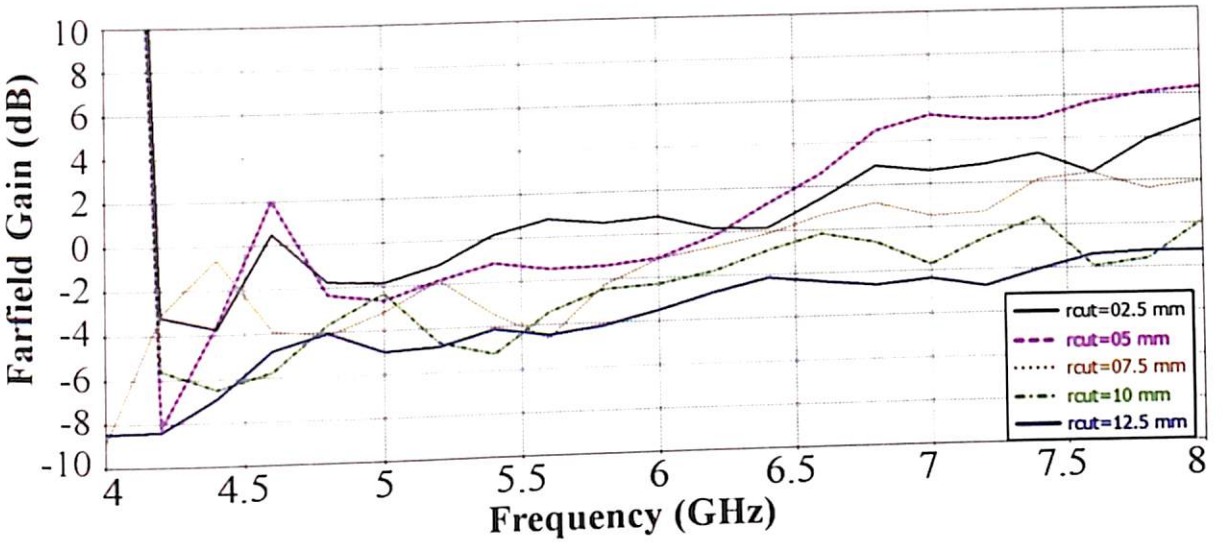

(a) Simulated maximum gain over frequency for different values of *rcut* with square ground plane (33.33×33.33 mm^2).

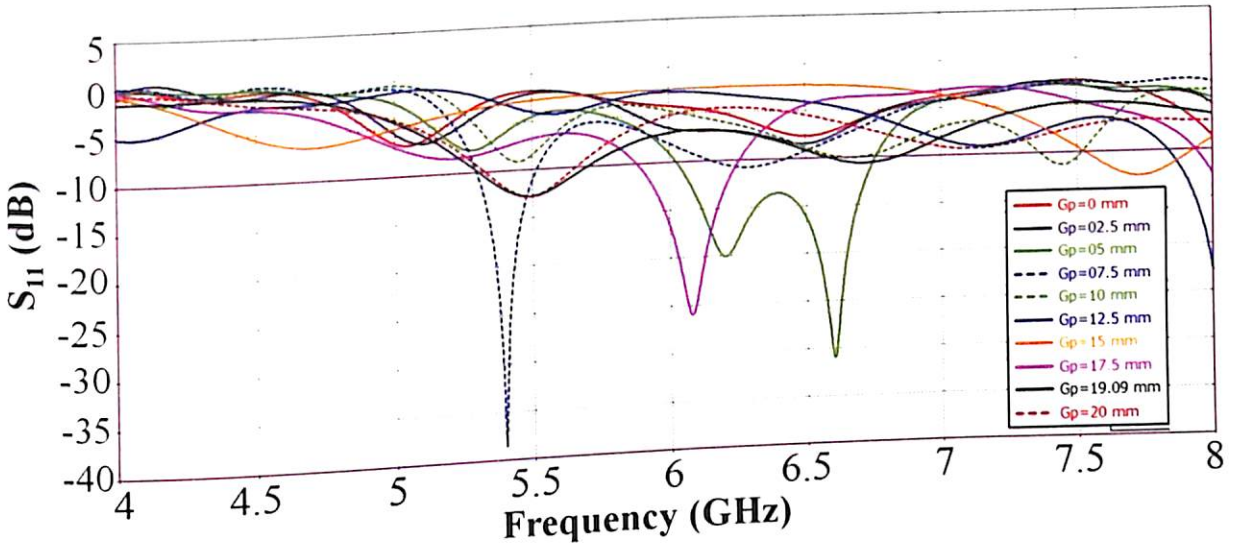

(b) Simulated Reflection coefficients (S_{11}) for different values of G_p when feed point is at 14 mm and *rcut* is 2.5 mm.

Figure 3.2. Effect of varying *rcut* and G_p.

The optimum value of the hexagonal slot can be obtained using technique proposed in (Joshi 2015c) which describes how the gain (in dB) varies with *rcut*. The *rcut* plays a significant role on gain characteristics of the patch antenna. To study the effect of the *rcut*, a

parametric study is again performed by varying the slot size by changing *rcut* as shown in Figure 3.2(a).

The effect on gain (in dB) by increasing the value of *rcut* is displayed in Figure 3.2(a). In all simulations done, the circumradius of hexagonal shaped patch is 15 mm. Since, the gain at 5.5 GHz is highest when *rcut* is 2.5 mm as shown in Figure 3.2(a), the value of *rcut* chosen here is 2.5 mm. To optimize the reflection coefficient (in dB) further at 5.5 GHz, the ground plane is reduced as the length, width and position of ground plane of a patch antenna plays a significant role in its performance. Figure 3.2(b) displays the effect of G_p on reflection coefficient (in dB) when *rcut* is 2.5 mm, where G_p is defined as reduction in length of ground plane i.e. by increasing G_p, length of ground plane decreases. By reducing the length of the ground plane, the patch capacitance is changed due to change in overlapping area of patch with the ground plane. It is observed that the optimum value of G_p at 5.5 GHz is 19.09 mm.

Simple *RLC* resonant equivalent circuit is used to model the hexagonal shaped patch antenna with hexagonal slot, as shown in Figure 3.3.

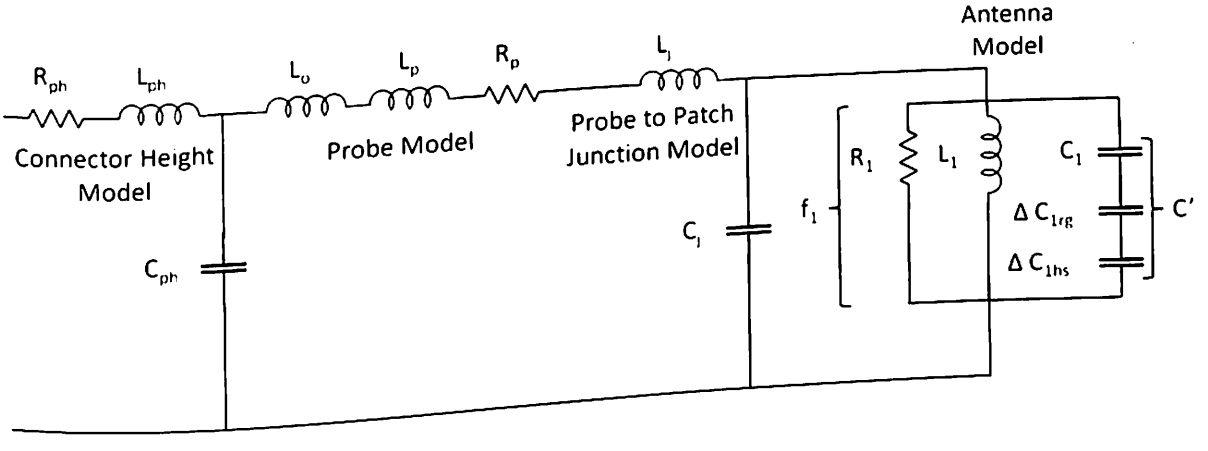

Figure 3.3. Equivalent Circuit model of the proposed antenna.

After applying equations given in (Garg 2001), lumped elements (*RLC*) can be obtained for different polygonal patch antenna, as given in chapter 2 by equations (2.1-2.3). The expression given in equation (2.1) is used to calculate C_1 for different effective overlapping

area, where C' is equivalent capacitance calculated for a series combination of C_n, ΔC_{nrg} (change in capacitance due to reduced ground), and ΔC_{nhs} (change in capacitance due to introduction of hexagonal slot), where, n is 1 and 2. The effective overlapping area (A_e) of the hexagonal patch with a full square ground is 584.57 mm^2 while capacitance (C_1) calculated using equation (2.1) is 7.42 pF. The effective overlapping area (A_e) of hexagonal patch with the reduced ground (reduced by a factor of G_p =19.09 mm) and after introducing the hexagonal slot is 242.81 mm^2 and capacitance (C') is found to be 3.08 pF using equation (3.1).

$$\frac{1}{C'} = \frac{1}{C_n} + \frac{1}{\Delta C_{nrg}} + \frac{1}{\Delta C_{nhs}} \tag{3.1}$$

The hexagonal patch inductance (L_1 = 0.270 nH) is calculated using equation (2.2) for FR-4 substrate height (h) of 1.5 mm and probe diameter (d) of 1.24 mm at frequency, f_1 = 5.5 GHz. Similarly, hexagonal patch resistance (R_1 = 131.4 Ω) is calculated using equation (2.3) by substituting Q = 13.97 which calculated using (Garg 2001).

The rigorous approach of coaxial probe modeling and analysis is given in (Garg 2001) (Pozar 2014). Consider the equivalent circuit model of a probe fed polygonal shaped patch antenna as shown in Figure 3.3. The input impedance (Z_{11}) of a patch antenna is determined for a RLC resonator near its resonant frequency i.e. 5.5 GHz. The SMA connector or probe can be modeled in three sections i.e. probe height model (Pozar 2014), probe model (Garg 2001) and probe to patch junction model (Pozar 2014). The probe height model can modeled as coaxial transmission line model by series resistance (R_{ph} = 0.0644 Ω), series inductance (L_{ph} = 2.417 nH) and shunt capacitance (C_{ph} = 0.4181 pF). The probe model can modeled as by series inductance (L_o = 25.071 pH and L_p = 0.607 nH), resistance (R_p = 16.28 Ω) as shown in Figure 3.3. The series inductors (L_o and L_p) used to model the feed probe, are proportional to the height of the dielectric substrate. The junction between probe and the polygonal patch

can be modeled as shunt capacitance (C_j = 0.1302 pF), series inductance (L_j = 2.11 nH). The impedance of a probe height model and probe junction model can be calculated using the equations given in (Pozar 2014), while the impedance of the probe model can be calculated using equations given in (Garg 2001).

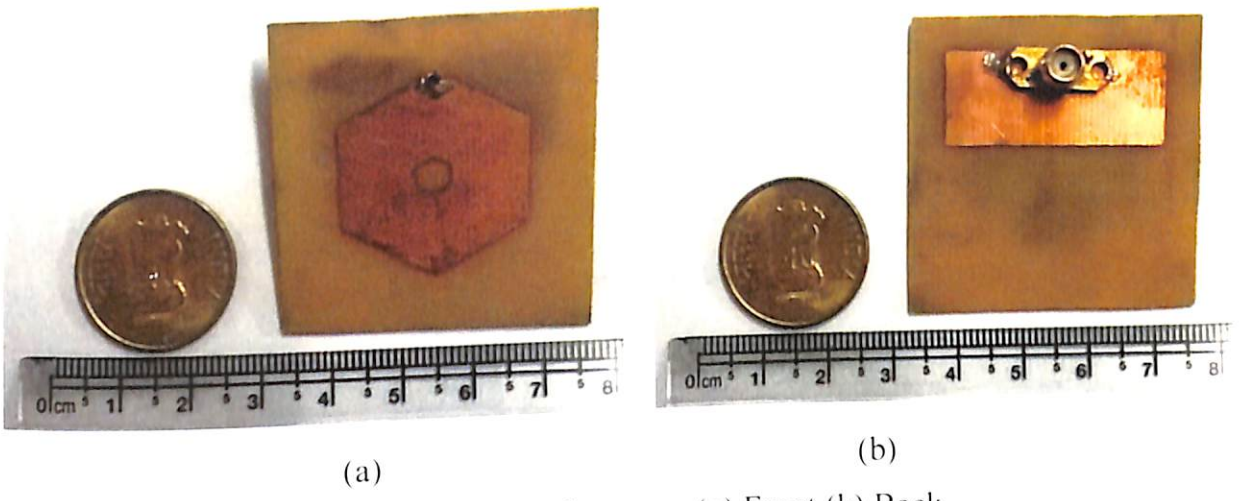

(a) (b)

Figure 3.4. Photograph of the fabricated antenna (a) Front (b) Back.

The picture of the fabricated hexagonal shaped patch antenna with hexagonal slot and reduced ground is shown in Figure 3.4. The fabricated antenna has an overall size of around 0.8148 λ_o × 0.8148 λ_o, which is very compact. To study the effect of hexagonal slot and reduced ground on reflection coefficient (S_{11}) and impedance (Z_{11}) for the proposed antenna, the simulated results obtained from CST MWS are analyzed and compared with measurements collected from Keysight Technologies Vector Network Analyzer (N9928A).

The reflection coefficient (S_{11}) result obtained from equivalent circuit model with probe is also compared with simulated and VNA measured results. The results from VNA, equivalent circuit model and the full-wave simulation using CST MWS are compared in Figure 3.5. The simulation and measurement results show a similar band from 5.29 to 5.71 GHz (~400 MHz). The second frequency at 6.7 GHz in equivalent circuit model is due to the probe to patch junction capacitance. Circuit modeling as shown in Figure 3.3 helps in identifying the spurious frequency 6.7 GHz.

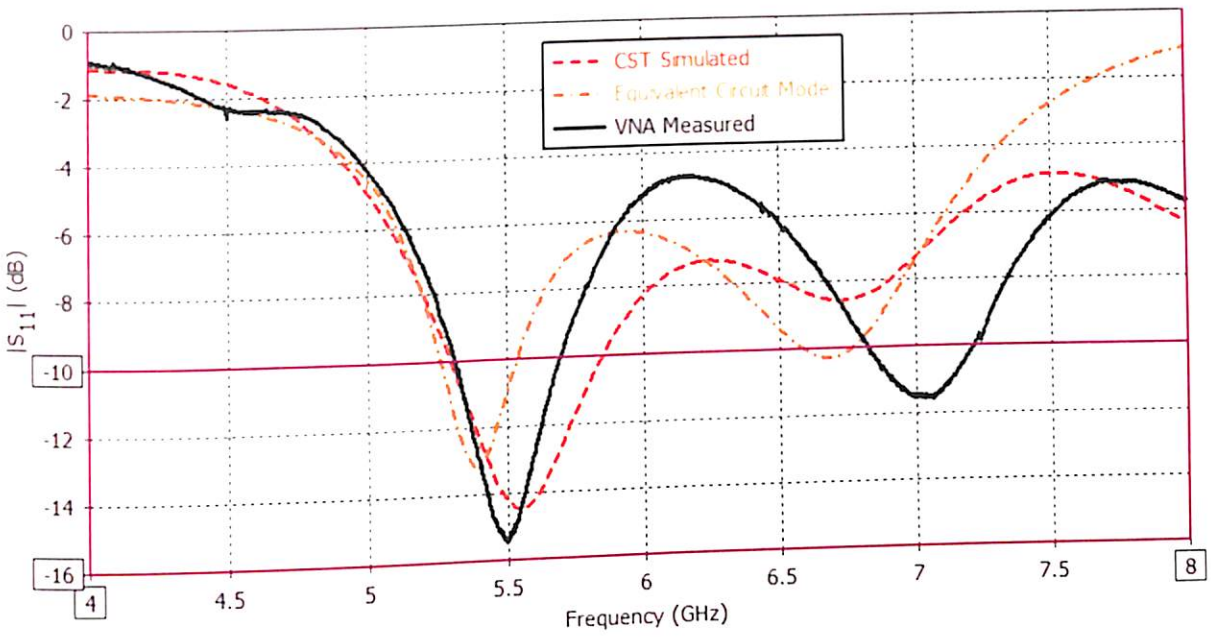

Figure 3.5. Measured Reflection coefficient (in dB) (S_{11}).

A significant objective of the patch antenna design is to match impedance to transmission line. The impedance (Z_{11}), real part and imaginary part, obtained from measurements and simulation are compared and presented in Figure 3.6 respectively. The optimum value of simulated Z_{11} (real and imaginary) between 5.27 to 5.71 GHz is at 5.5 GHz which is approximately $53.92 + 18.94j\ \Omega$ in the operating band as shown in Figure 3.6. Measurement results of the fabricated antenna from VNA show the optimum value of Z_{11} at 5.5 GHz to approximately $56.43 + 17.25j$ in the operating band between 5.29 to 5.71 GHz.

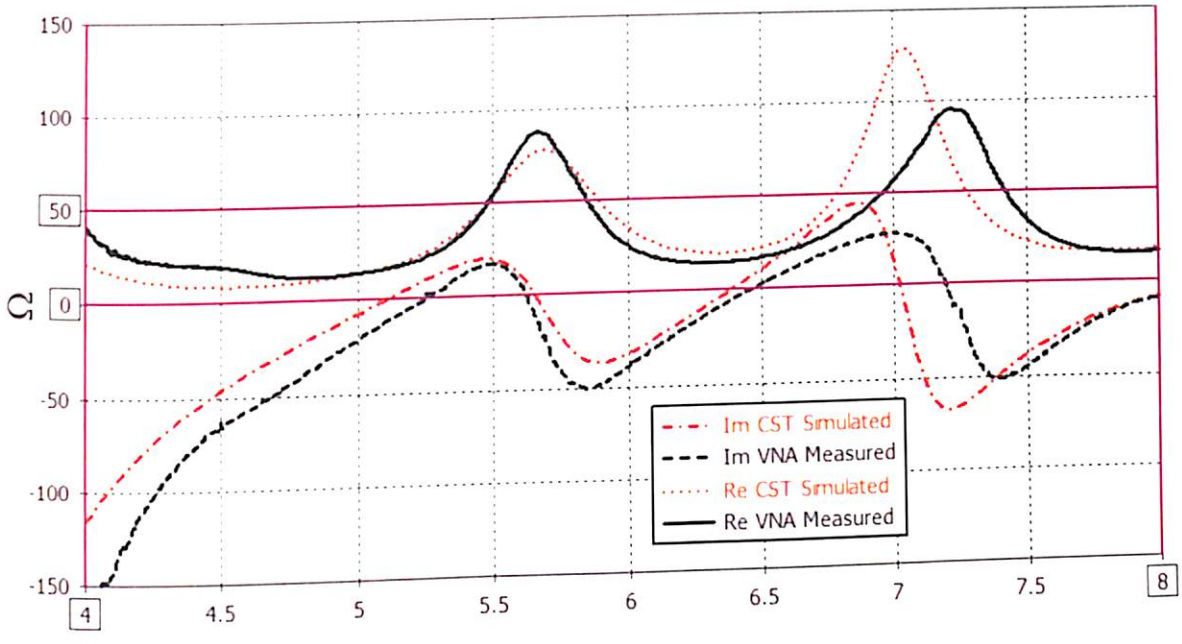

Figure 3.6. Measured Impedance Real and Imaginary part (Z_{11}).

A loop is observed in Smith Chart within the operating frequency band in both simulation and measurement results as shown in Figure 3.7. The loop is rotated anticlockwise towards the capacitive region as shown in Figure 3.7(b), due to the capacitive effect of the small air gap between the connector flanges and the antenna. The actual probe effect is seen in measured result shown in Figure 3.7(c). The probe model chosen in equivalent circuit model results in impedance values closer to measurements as compared to simulation. The main lobe Axial Ratio (AR) through CST simulation at frequency 5.5 GHz is found to be 5.84 dB $\geq$ 2 dB that suggests linear polarization.

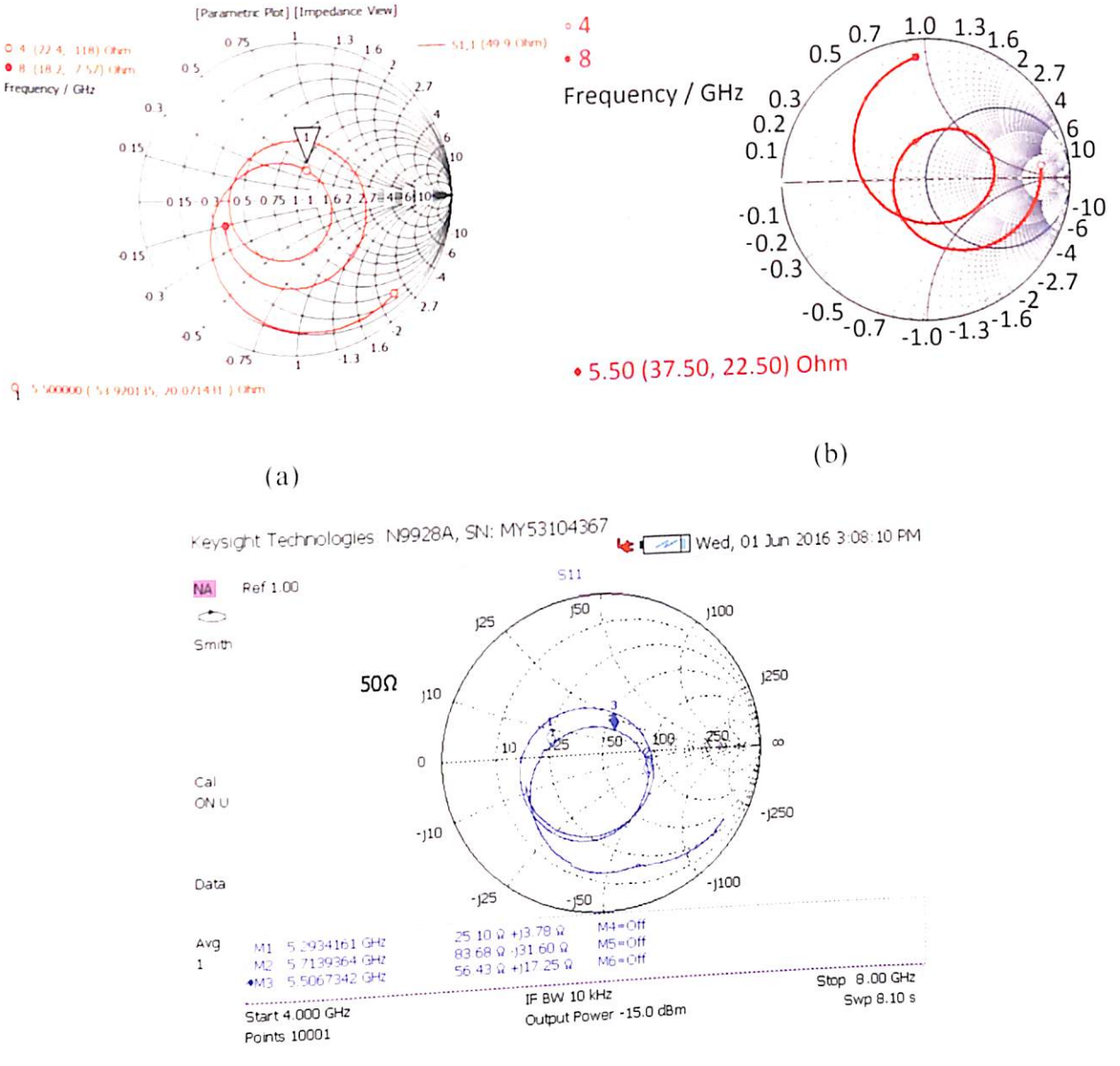

Figure 3.7. Smith Chart for proposed antenna using (a) CST (b) Equivalent Circuit Model (c) VNA.

3.3. Adjacent Resonance Suppression in a Vertex-Fed Hexagonal C-Band Antenna

The structure of the proposed C-Band antenna designed at 5 GHz is shown in Figure 3.8. The antenna structure is developed on FR-4 substrate of thickness, h = 1.5 mm, with dielectric constant, ε_r = 4.3 and loss tangent, (tan δ) = 0.025 with an overall dimension of 46 × 46 mm^2 is used for proposed antenna design. The circumradius of patch, R = 17.5 mm and the ground

plane has an area of 37 × 39 mm^2 reduced to 9 × 39 mm^2. The patch size is around 0.58 λ × 0.51 λ at 5 GHz with a coinciding slot with a circumradius, r_{cut} = 3 mm.

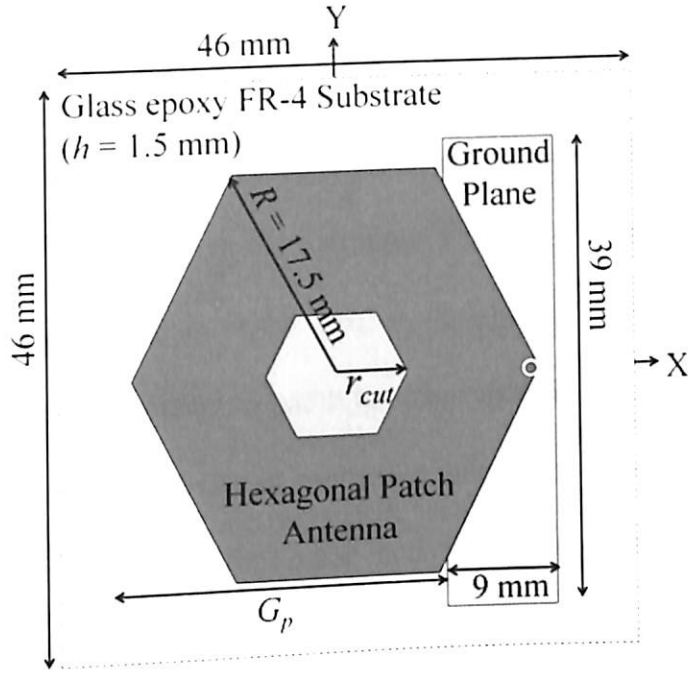

(a)

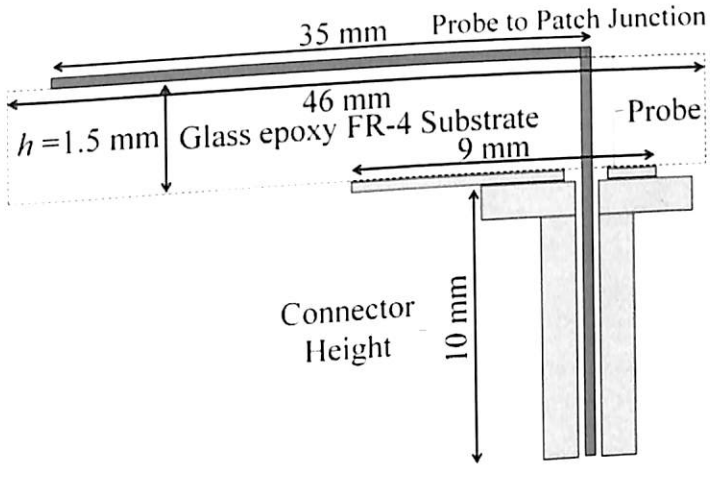

(b)

Figure 3.8. Hexagonal patch antenna structure (a) Layout with dimension (b) Side view.

The RF energy is fed through a SMA connector placed at the vertex of hexagon i.e. 17.5 mm from the patch centre. The pin radius of SMA connector is 0.62 mm, and radius of dielectric (Teflon) used with SMA connector is 2.08 mm. The outer conductor of SMA

connector has a radius of 2.57 mm with a height of 10 mm. The length of the ground plane is reduced by G_r = 28 mm to a narrower ground plane than the ground plane used in (Joshi 2016b). Presence of hexagonal slot increases current density in patch and improves gain slightly (Joshi 2015c).

To explain the mechanism of the proposed antenna with suppressed spurious frequency, an equivalent circuit is modeled using typical mathematical and analytical simulation platform and presented in Figure 3.9. The complex probe model consists of the connector height model, the probe model and the probe to patch junction model. The inductance due to probe height, L_{ph} is due to the inner conductor of the probe height with resistance R_{ph}, while C_{ph} is the capacitance developed between the inner and outer conductor separated by Teflon dielectric of the probe height. The optimized ground does not overlap with the hexagonal slot in the patch, model of Figure 3.3 is modified in terms C' and modified model is presented in Figure 3.9, and equation (3.1) is reduced to equation (3.2).

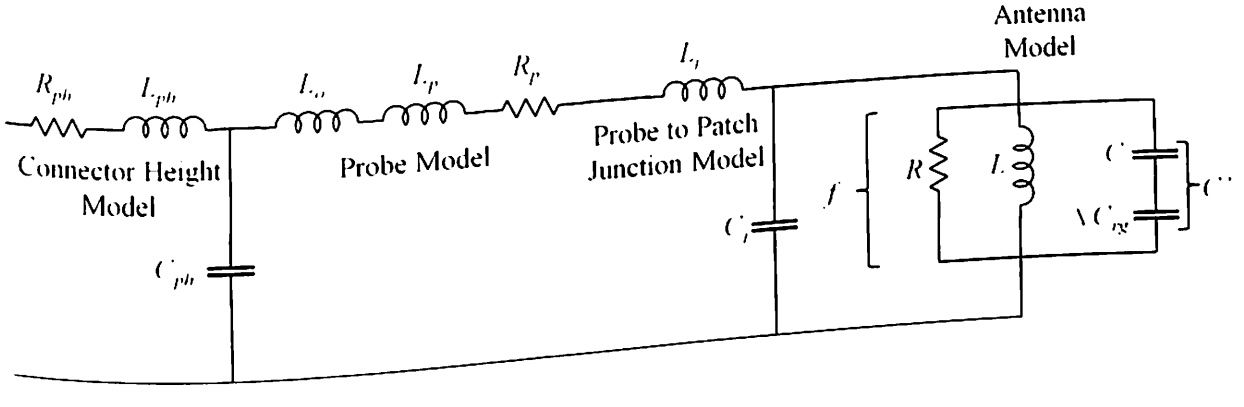

Figure 3.9. Equivalent circuit model of the designed antenna.

$$\frac{1}{C'} = \frac{1}{C_n} + \frac{1}{\Delta C_{nrg}} \tag{3.2}$$

The probe model is due to the inner conductor of the probe which is inserted in the substrate with height h via hole to connect the patch. The pin with length equal to h will have inductance (L_o + L_p) and resistance (R_p). The probe to patch junction have a series inductance

L_j and a shunt capacitance C_j. The proposed antenna is modeled as a simple parallel RLC circuit which resonates at a frequency f = 5 GHz as shown in Figure 3.9. The capacitance (C = 10.098 pF) is due to full ground overlapping with the hexagon. Due to reduced ground plane (RGP), the capacitance C is reduced by a factor modeled as a capacitor in series (ΔC_{rg} = 1.625 pF) to form C'. The values of the lumped circuit elements are indicated in Table 3.1.

Table 3.1. Values of Lumped Elements of Equivalent Circuit Model

Model	Parameters	Values
Antenna Model	C'	1.4 pF
	L	0.72 nH
	R	226.27 Ω
Connector height Model	R_{ph}	0.06 Ω
	L_{ph}	2.42 nH
	C_{ph}	0.46 pF
Probe Model	L_o	21.6 pH
	L_p	0.63 nH
	R_p	14.8 Ω
Junction Model	L_j	5 nH
	C_j	0.20 pF

The picture of the prototype of the designed antenna is shown in Figure 3.10. The scattering parameter, S_{11} of developed antenna is measured on a vector network analyzer (VNA) (Keysight N9928A) to observe the effect of RGP on S_{11}. The S_{11} measurements from VNA are shown in Figure 3.11 and compared with that observed in (Joshi 2016b).

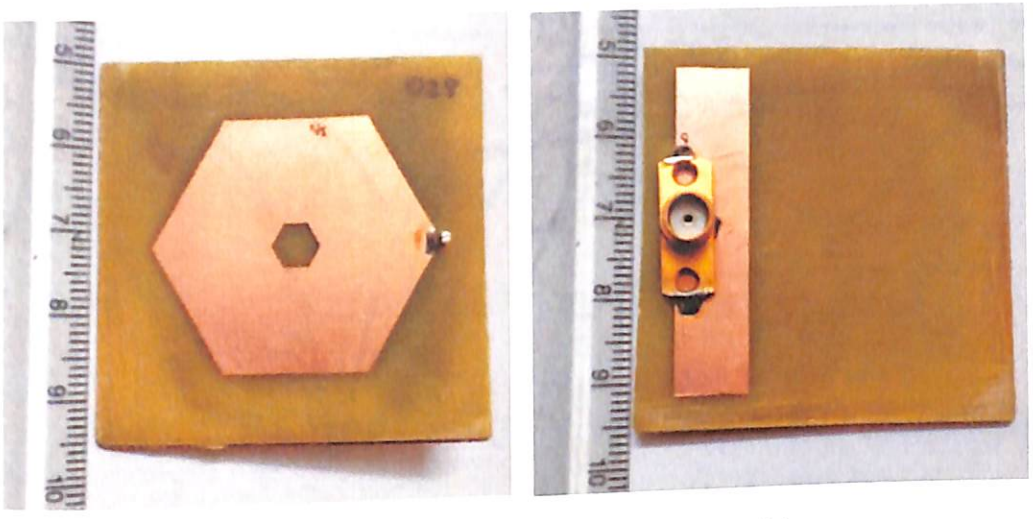

(a) (b)

Figure 3.10. Picture of the designed antenna (a) Front view (b) Back View.

Spurious frequency at 7 GHz as observed in (Joshi 2016) is evidently suppressed as shown in Figure 3.11 due to increase in G_p. Suppression of 7 GHz is observed when ground plane is reduced. Thus, RGP may be used as a effective technique to suppress a successive higher order mode, if required in certain application. A frequency shift from 5.5 GHz to 5 GHz is also observed in Figure 3.11 due to increase in circumradius of patch from 15 mm (Joshi 2016) to R = 17.5 mm in proposed antenna. The change in radial distance R is done here, in this work to target indoor WLAN applications. The measured return loss of proposed antenna display a band from 4.8 to 5.4 GHz (~ 600 MHz). The measured S_{11} results are also compared with the simulation results and equivalent circuit model result as shown in Figure 3.11. The simulated and equivalent circuit model also shows a similar -10 dB band from 4.79 to 5.29 GHz (~ 500 MHz).

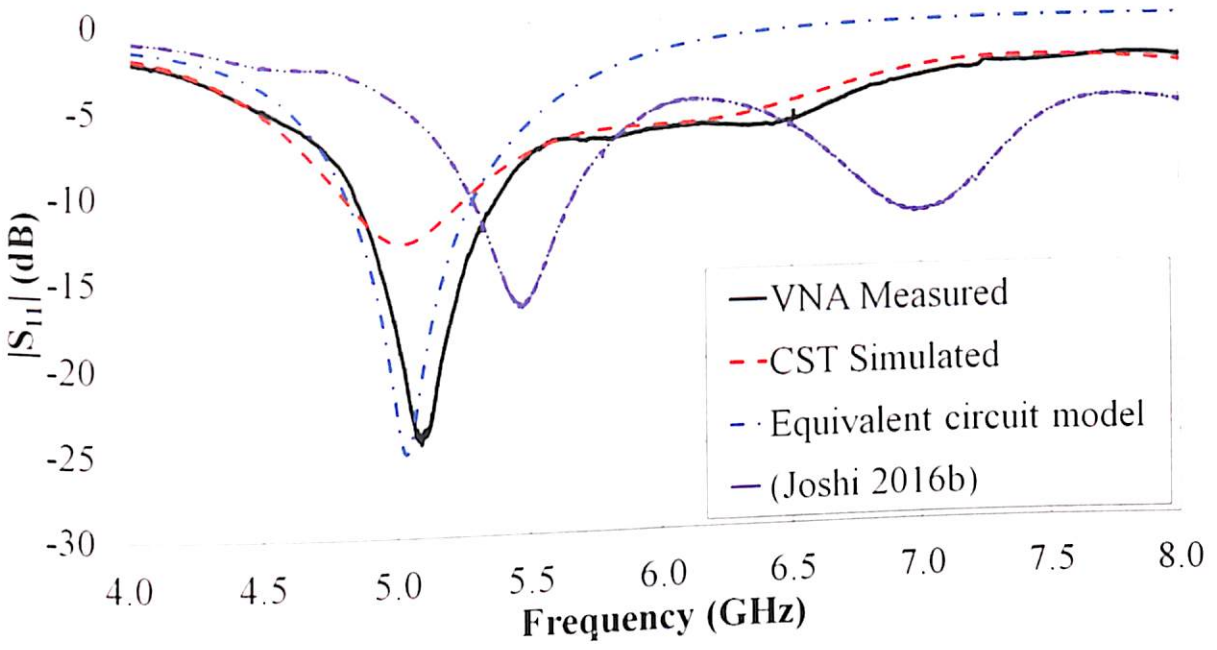

Figure 3.11. Scattering parameter, $|S_{11}|$ (in dB)

The variation of the input impedance with frequency on the Smith Chart, with results obtained from measured, simulated and modeled antenna is shown in Figure 3.12. A loop in the capacitive region of Smith Chart is observed within the operating bandwidth as shown in Figure 3.12. The resonant frequency observed in circuit modeling is very close to that observed during measurements. It can be observed from the Smith Chart that measurements reflect low reactance than observed in simulated results at 5 GHz. Although vertex-feeding is not a suitable location for matched impedance but impedance, Z_{11} is found to be 53.37 - 5.2j Ω when measured on VNA at 5 GHz due to RGP. While the simulated and equivalent circuit model reflects the value of input impedance as 45.26 - 21j Ω and 55 + 0j Ω respectively at 5 GHz.

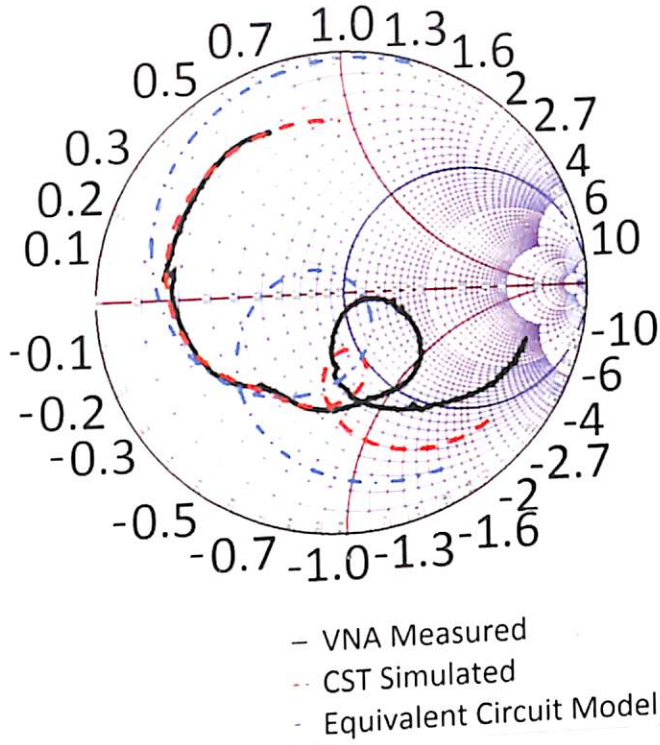

Figure 3.12. Variation of the input impedance of the proposed antenna on Smith Chart.

The modal characteristics of the proposed antenna is also analyzed and observed using the surface current density with four different phase of excitation signal i.e. 0°, 90°, 180° and 270° at resonating frequency of 5 GHz and is displayed in Figure 3.13. The surface current density analysis suggest that the maximum current density is observed at the overlapping area of the hexagon with the ground. The surface current vector is along the two edges within the overlapping area of the patch is shown in Figure 3.13(a). The vector moves on surface of the patch from feeding vertex to the nearest vertex and returns back to the feeding vertex again through edges forming a loop at 0° phase of the excitation signal. The vectors follow opposite direction with the phase reversal of 180°, as observed from Figure 3.13(c). At 90° phase, the surface current vectors are creating three loops along the three vertices of the hexagon overlapping with the ground as reflected in Figure 3.13(b). Similar effect is observed at 270° phase in Figure 3.13(d), where vector directions are opposite to that of 90° phase.

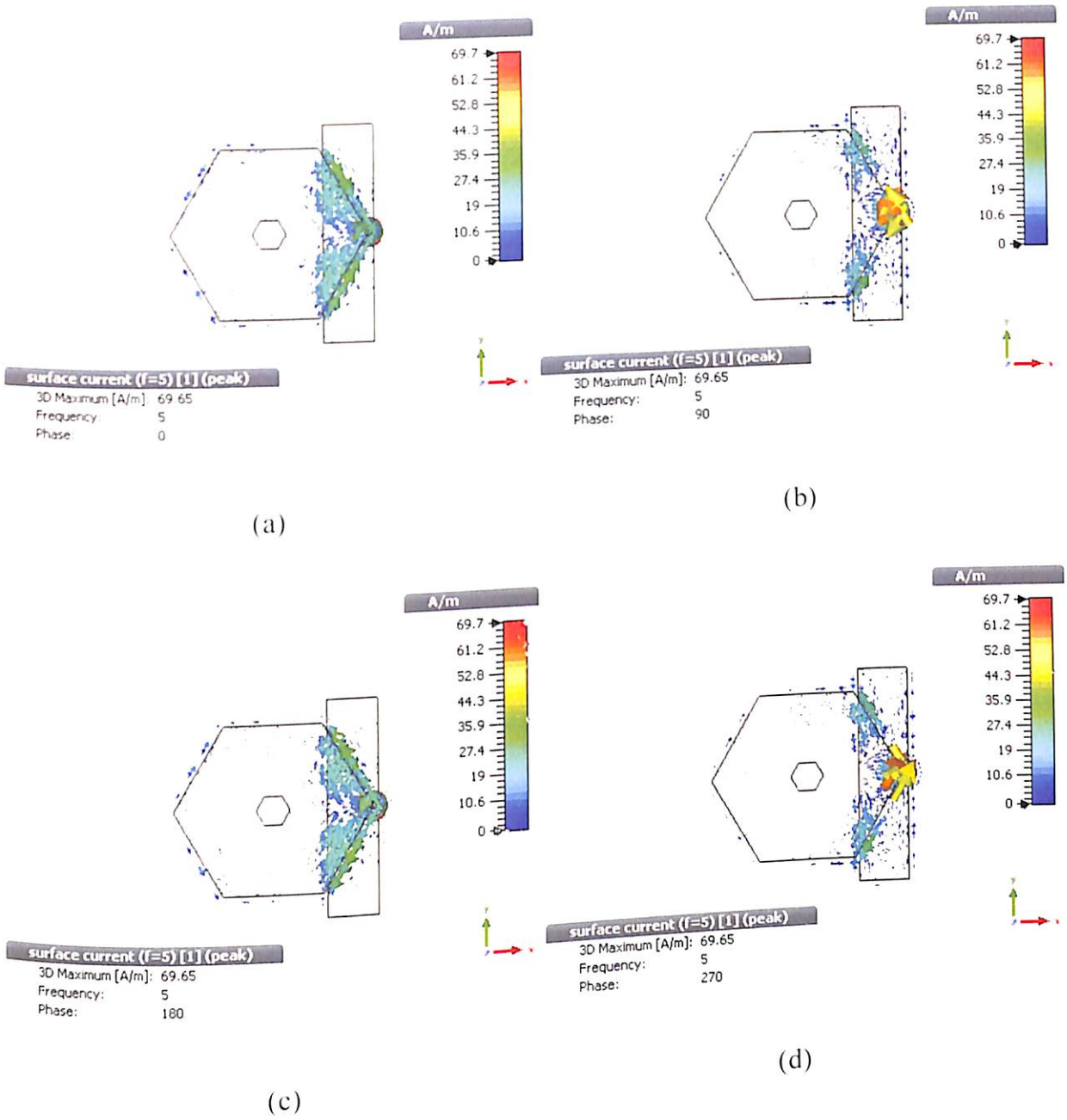

Figure 3.13. Surface current density of the designed antenna at 5 GHz at different phase of excitation signal (a) 0° (b) 90° (c) 180° (d) 270°

3.4.Vertex-Fed Hexagonal X-band Antenna

The design of a compact regular hexagonal shaped patch antenna with reduced ground is shown in Figure 3.14 and is optimized at a lower frequency of X-Band. The proposed antenna in Figure 3.14 uses a glass epoxy FR-4 substrate ($\varepsilon_r = 4.3$, $\tan\delta = 0.025$) of thickness 1.5 mm with dimension of 32×33.5 mm^2.

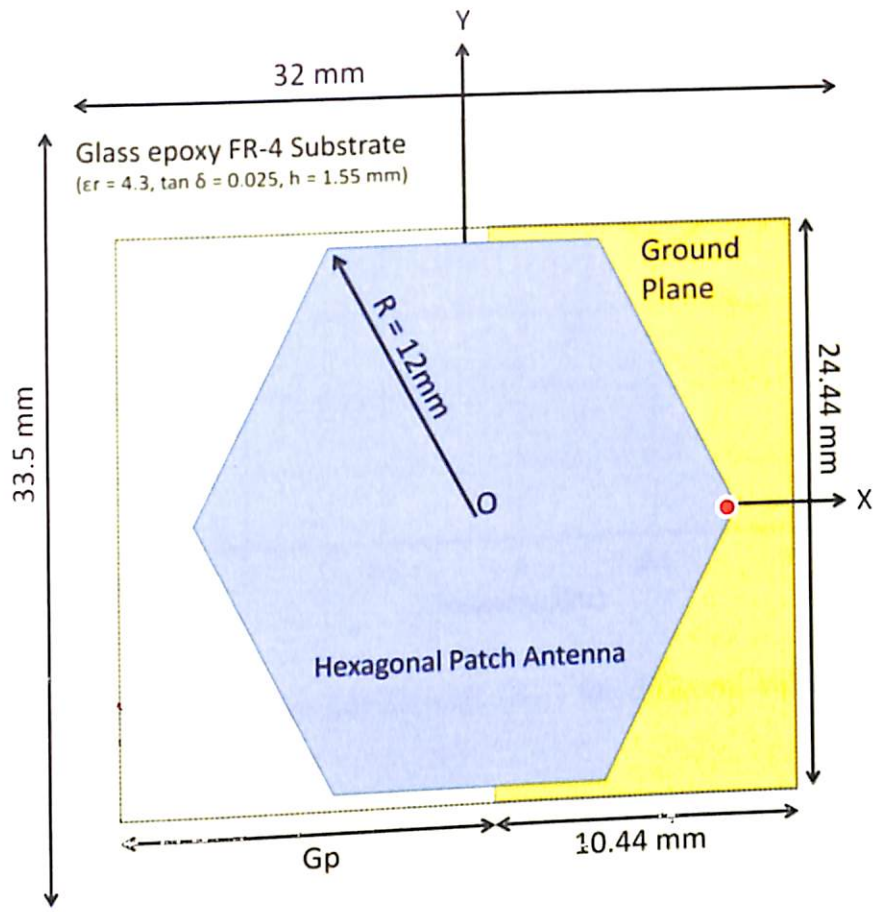

Figure 3.14. Schematic of the proposed hexagonal shaped patch antenna with reduced ground.

The dimension of the ground plane is 10.44 × 24.44 mm^2. In terms of the wavelength of the resonance frequency, the hexagonal shaped patch size is around 0.6960 λ_o × 0.6027 λ_o. The antenna is fed through a probe near the vertex at a distance of 10 mm from center of patch. The radii of the SMA connector are 0.805 mm, 2.22 mm, 3 mm for center pin, SMA Teflon, and outer conductor respectively, and the height of SMA connector is 10 mm.

The length, width and position of ground plane of a patch antenna play a significant role in its performance. To study effect of the ground reduction, a parametric study is performed by reducing the ground by a factor 'Gp' as shown in Figure 3.14. Gp is defined as reduction in length of ground plane i.e. by increasing Gp, length of ground plane decreases. Figure 3.15, Figure 3.16 and Figure 3.17 shows the effect on reflection coefficient and impedance (real and imaginary part) respectively by increasing value of Gp.

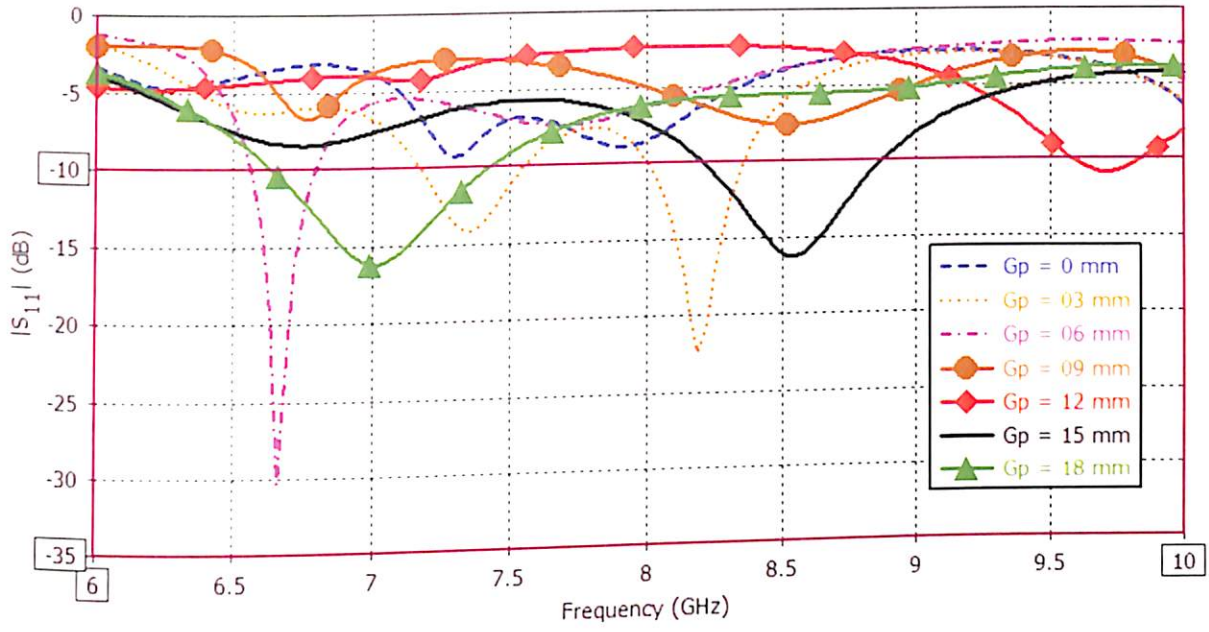

Figure 3.15. Simulated Reflection coefficients (S_{11}) for different values of Gp when feed point is at 10 mm.

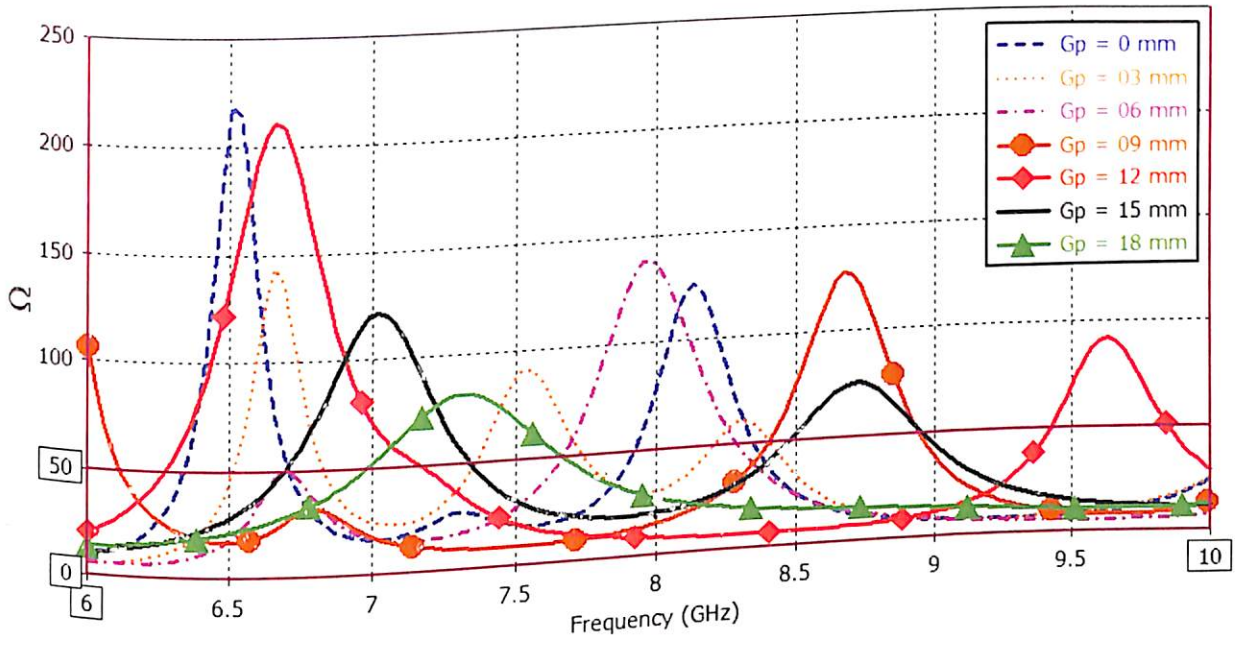

Figure 3.16. Simulated Re(Z_{11}) for different values of Gp when feed point is at 10 mm.

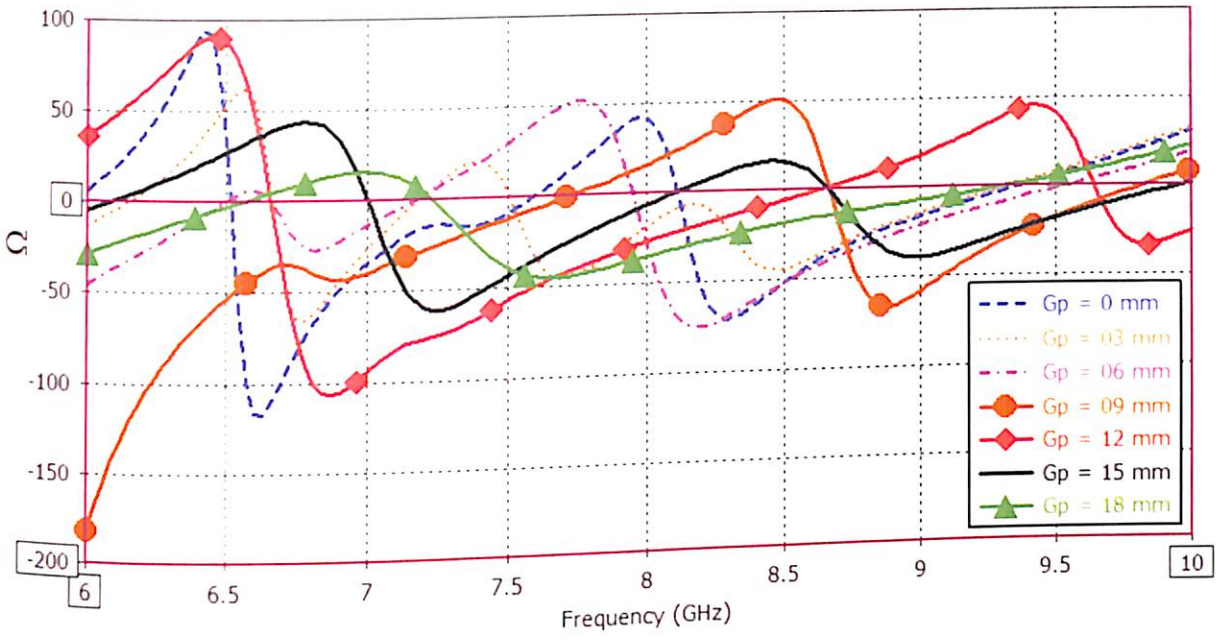

Figure 3.17. Simulated $Im(Z_{11})$ for different values of Gp when feed point is at 10 mm.

In all simulations done for parametric analysis, the circum-radius of hexagonal shaped patch is 12 mm. It was observed that the resonant frequency can be pushed up by reducing the ground to a lower frequency of X-Band. By reducing the length of the ground, the patch capacitance (C') is changed due to change in the overlapping area of patch with the ground. Due to change in the overlapping area the resonating frequency shifts towards higher range as shown in Figure 3.15. It is observed that when Gp is equal to 15 mm, the operating bandwidth is higher than when Gp is equal to 3 mm. Thus, optimum value of 14 mm is chosen for Gp to develop the antenna.

The hexagonal shaped patch antenna can be modeled as a simple *RLC* resonant equivalent circuit, as shown in Figure 3.18. Note that the equivalent circuit model is obtained for the VNA measured resonating frequencies i.e 7.15 GHz (f_1) and 8.69 GHz (f_2). Lumped elements at a simple resonant circuit *RLC* can be obtained similarly as done for a E-patch in (Malekpoor 2015). After modification in equations given in (Malekpoor 2015), equations (2.1-2.3) are obtained for a hexagonal patch antenna. The expression given in equation (2.1) is used to calculate C', C_1 and C_2 for different effective overlapping area.

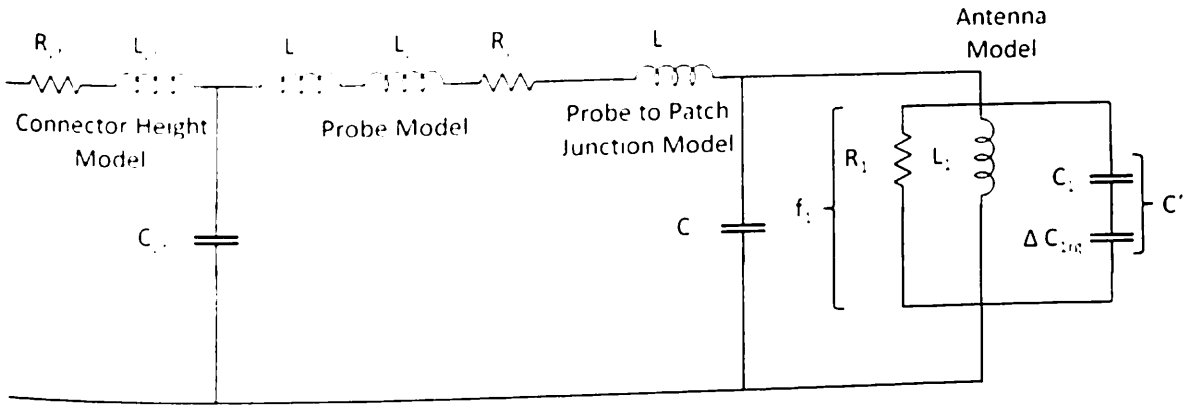

Figure 3.18. Equivalent Circuit model of the hexagonal shaped patch antenna with its probe feeding network.

The effective overlapping area (A_e) of the hexagonal patch with the full square ground is 374.12 mm^2 and capacitances ($C_1 = C_2$) calculated using equation (2.1) is 4.75 pF. The effective overlapping (A_e) of hexagonal patch area with the reduced ground (reduced by factor Gp =15 mm) is reduced to 150.03 mm^2 and capacitance (C') is found to be 1.90 pF using equation (2.1). Due to reduction in the ground, the value of capacitance of the hexagonal patch is reduced. This effect can be modeled as the additional series capacitance (ΔC_n). The additional series capacitance (ΔC_{nrg}) of a hexagonal patch can be obtained from equation (3.2) and calculated using the formula given in equation (3.3).

$$\Delta C_{nrg} = \frac{C_n \times C'}{C_n - C'} \tag{3.3}$$

where, n is the number of resonating frequencies and its value is 1 and 2. The value (ΔC_n = 3.18 pF) of the additional series capacitance of the hexagonal patch using equation (3.3) is indicated in Figure 3.18. The hexagonal patch inductance (L_1 = 0.26 nH and L_2 = 0.18 nH) calculated using equation (3.3) for FR-4 substrate with substrate height (h) of 1.5 mm and probe diameter (d) of 1.24 mm for the frequencies 7.15 GHz (f_1) and 8.69 GHz (f_2) as shown in Figure 3.18. Similarly, hexagonal patch resistance (R_1 = 461.29 Ω and R_2 = 377.63 Ω) is calculated using equation (2.2) by substituting Q = 39.26 which calculated using (Garg 2001).

The input impedance (Z_{11}) of a patch antenna of equivalent circuit model shown in Figure 3.18 is determined for a *RLC* resonator near its resonant frequencies i.e. 7.15 GHz and 8.69 GHz. The series inductors (L_o = 0.58 nH and L_p = 0.04 nH) of the SMA connector or feed probe, and is proportional to the height of the dielectric substrate (h). The SMA connector or probe can be modeled by series inductance (L_o and L_p), resistance (R_p = 25.73 Ω) and parallel capacitance (C_o = -0.06 pF) with other hexagonal shaped patch antenna lumped RLC elements as shown in Figure 3.18. The impedance of a SMA connector or the feed probe can be calculated using the formula given in (Garg 2001).

Figure 3.19. shows a picture of a developed hexagonal shaped patch antenna with reduced ground. The overall size of the hexagonal shaped patch antenna is around 0.9280 λ_o × 0.9715 λ_o, which is very compact.

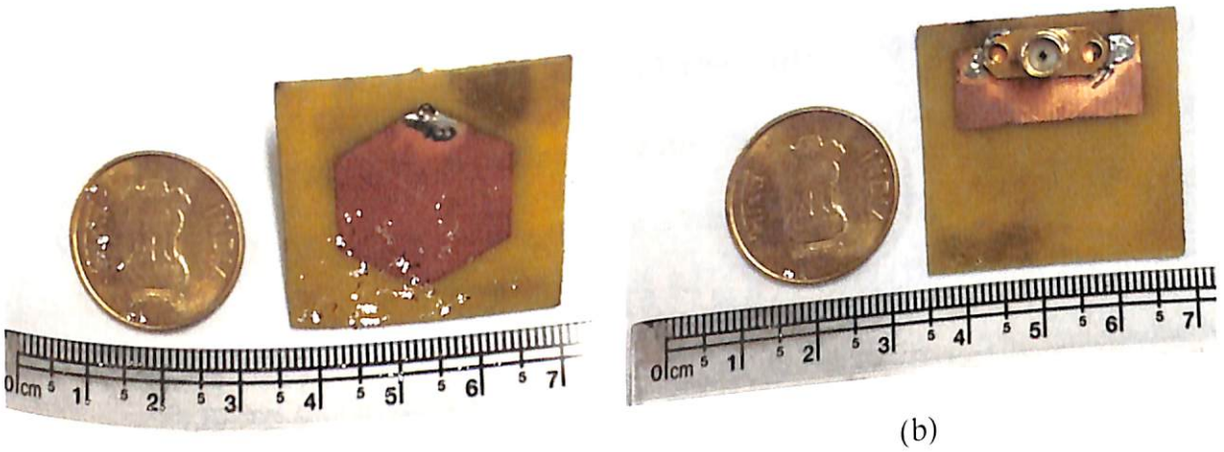

(a) (b)

Figure 3.19. Photograph of the fabricated hexagonal shaped patch antenna with reduced ground (a) Front (b) Back

The simulated results obtained are analyzed and compared with Keysight Technologies Vector Network Analyzer (N9928A) results to study the effect of reduced ground on reflection coefficient (S_{11}), voltage standing wave ratio (VSWR) and impedance (Z_{11}) for a hexagonal shaped patch antenna.

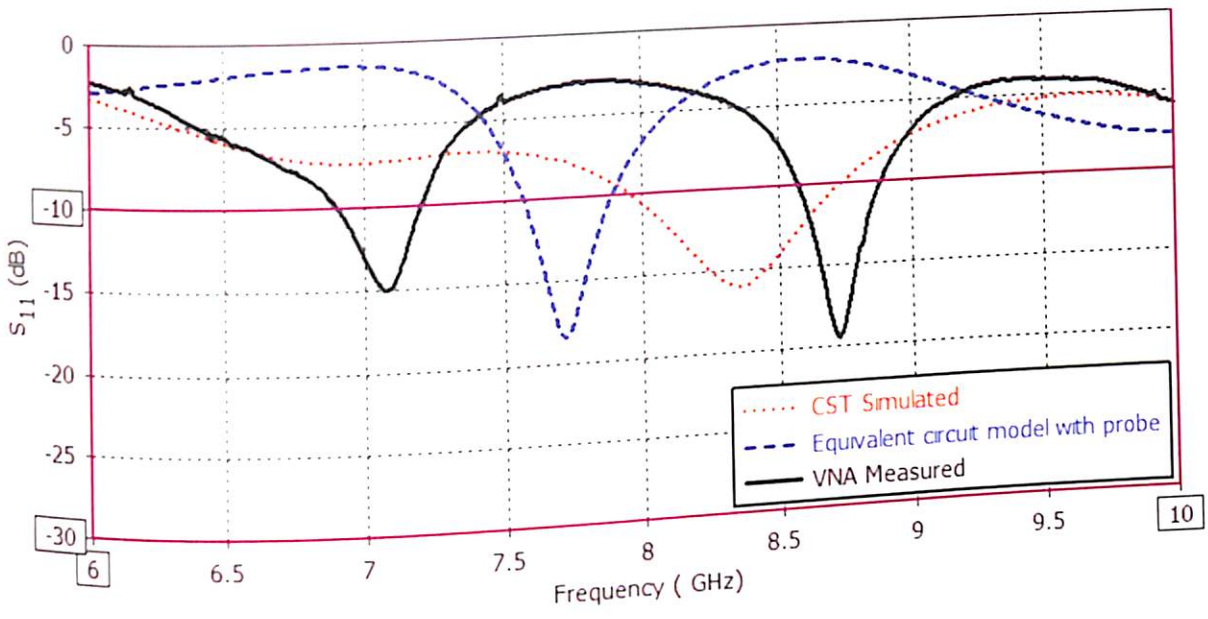

Figure 3.20. Measured Reflection coefficient (in dB) (S_{11}).

The results obtained from equivalent circuit model with and without probe are used to compare reflection coefficient (S_{11}) with simulated and VNA measured results. The reflection coefficient of the antenna is measured using VNA and is plotted in Figure 3.20. Figure 3.20 compares results from equivalent circuit model with feed probe and the full-wave simulation using CST MWS. The simulation results shows a band from 7.95 to 8.73 GHz (778 MHz) while VNA measured result shows a band from 8.57 to 8.89 GHz (321 MHz). The measured VNA bandwidth is less due to the inductance introduced by coaxial feed. The same inductive effect can be verified from VNA measured Smith Chart with a big loop (at 8.69 GHz) in inductive region shown in Figure 3.22(c) while the simulation shows a big loop (8.35 GHz) with major part in capacitive region. It proves that SMA connector is responsible for narrowing down the impedance bandwidth.

Matching impedance to transmission line is one of the significant objectives for a patch antenna design. The impedance real part and imaginary part are measured and compared with simulated results as presented in Figure 3.21 respectively.

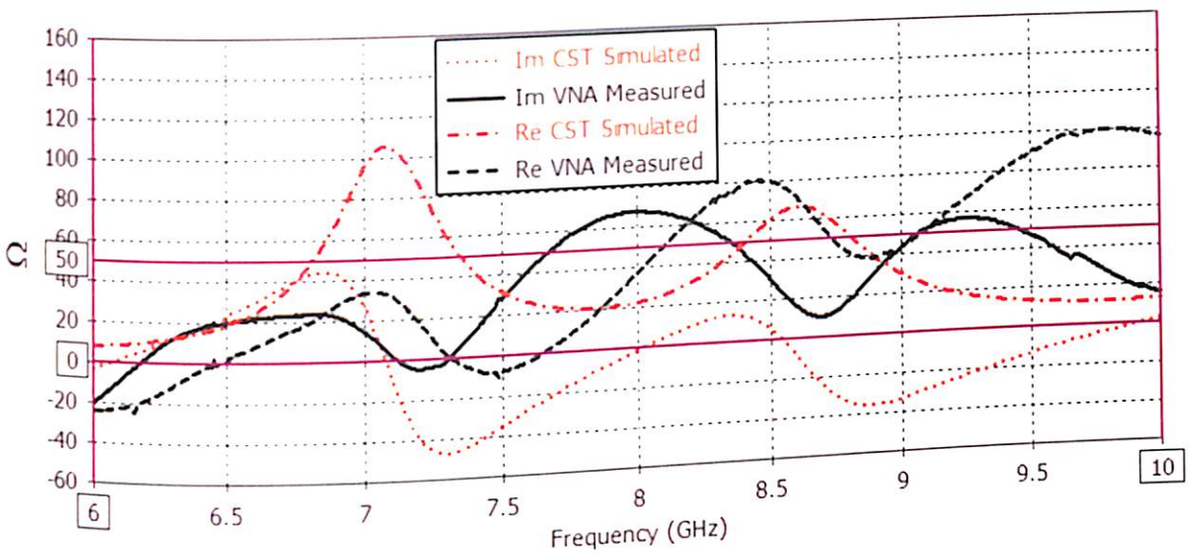

Figure 3.21. Measured Impedance Real and Imaginary part (Z_{11}).

It is observed that values of Z_{11} between 7.95 to 8.73 GHz is optimum at 8.35 GHz to approximately $50 + 9.9j\ \Omega$ in the operating band for hexagonal shaped using simulated real and imaginary Z_{11} as shown in Figure 3.21. Measurements using VNA shows that the value of Z_{11} is optimum at 8.69 GHz to approximately $51.6 + 10j\ \Omega$ in the operating band of the fabricated hexagonal patch antenna between 8.57 to 8.89 GHz.

The Smith Chart of hexagonal shaped patch antenna is shown in Figure 3.22. In the operating frequency band, in both simulated and measured Smith Chart, a loop is observed as shown in Figure 3.22(a) and (b). Simulated results show a large loop in the capacitive region, while the measured results show two loops whose cusp are at 7.15 GHz and other at 8.69 GHz frequencies. Smith Chart for Hexagonal patch antenna with probe using Equivalent circuit model is shown in Figure 3.22(b). The probe model in CST is less accurate so the maximum portion of the big loop representing the operating bandwidth is present in the capacitive region i.e. patch reactance dominates the results as shown in Figure 3.22(a). While, the probe model in equivalent transmission line modeling is more accurate as compared to CST hence the loop is rotated anticlockwise towards the inductive region as shown in Figure 3.22(b).

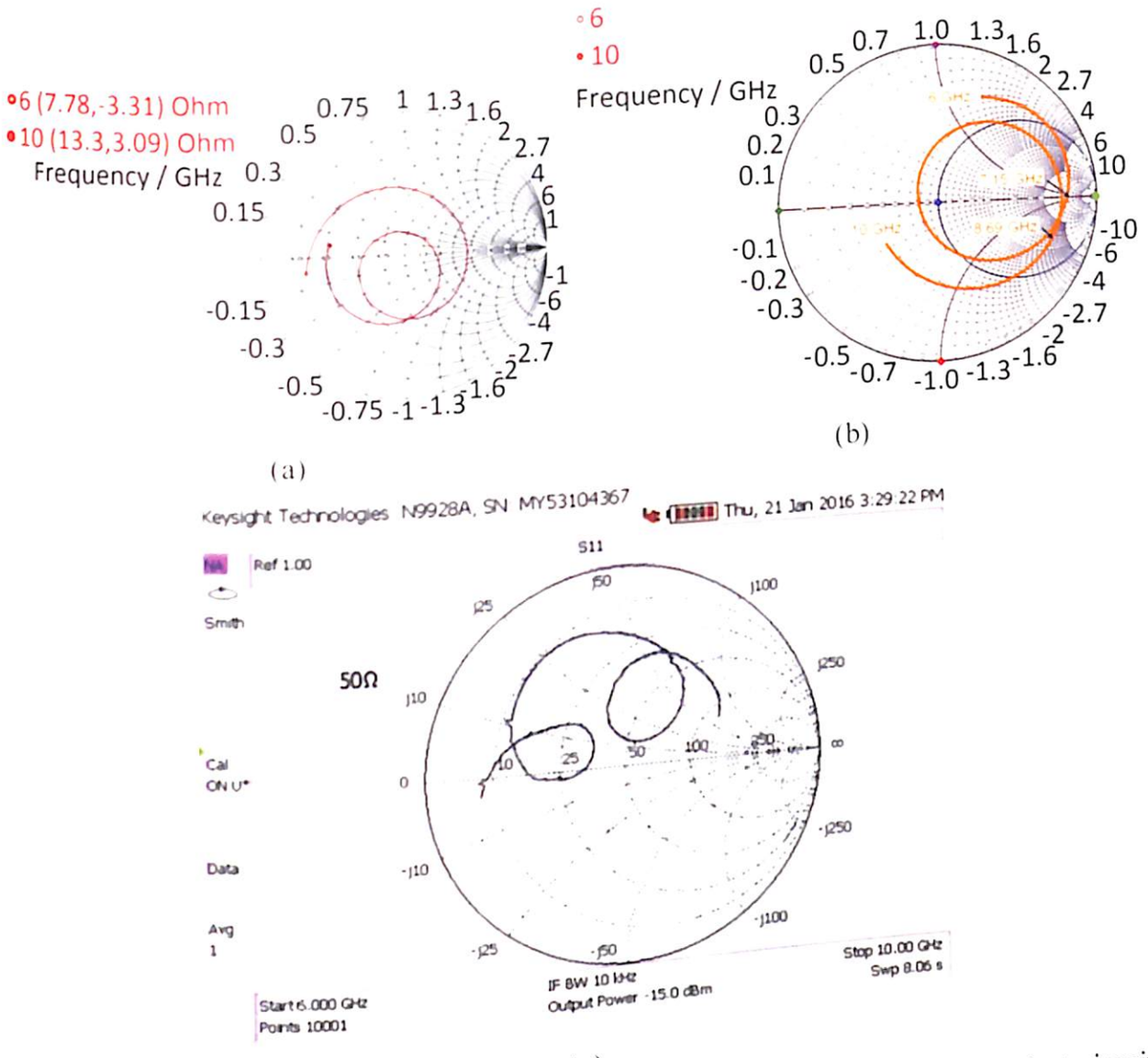

Figure 3.22. Smith Chart for Hexagonal patch antenna using (a) CST (b) Equivalent circuit model (c) VNA.

The actual probe effect is seen in measured result shown in Figure 3.22(b), where the loop is small and rotated anticlockwise direction fully in inductive region as compared to equivalent transmission line model.

3.5. Performance Comparison of Vertex-Fed Hexagonal Antennas

The vertex-fed hexagonal patch antennas with reduced ground are designed as shown in Figure 3.23(a) while the cross section along the x-axis is shown in Figure 3.23(b).

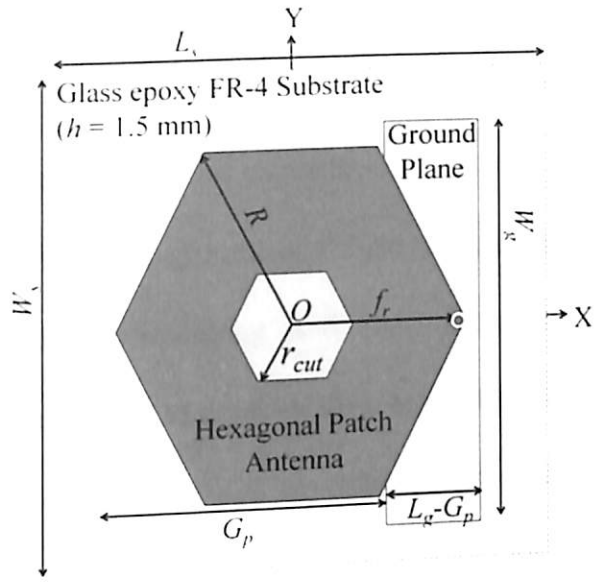

(a)

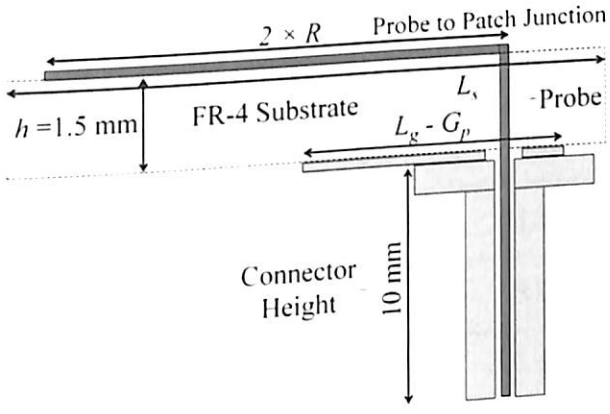

(b)

Figure 3.23. Proposed vertex fed hexagonal antenna with reduced ground (a) Schematic (b) Cross sectional view.

To understand the effect of reduced ground, three antenna prototypes are designed and fabricated. Dimensions of features used for all three antennas are shown in Table 3.2. In all antenna prototypes, substrate material FR-4 (ε_r = 4.3 and tan δ = 0.025) with height (h =1.5 mm) is used. In all antenna prototypes, standard sub-miniature (SMA) connector with a pin diameter of 1.24 mm is used to feed the hexagonal patch. The height of the outer conductor is 10 mm with radius 2.57 mm as shown in Figure 3.23(b). Since, first antenna prototype (Antenna 1) does not consist of the hexagonal slot while antenna prototypes, i.e. Antenna 2 and Antenna 3 are designed with a hexagonal slot. The values of radius of hexagonal slot

radius are indicated in Table 3.2. Dimensions of the hexagonal slot are optimized using method already suggested in (Joshi 2015c) which demonstrates small improvement of antenna gain too. While performing the experiments, the size of the antennas is varied to verify the performance of reduced ground at different resonances within the C-band. The approach to improve impedance matching is to vary the size of the ground plane while keeping the height of the dielectric (h) constant. The area of the hexagonal patch that overlaps with the ground plane reduces which results in variation of the patch capacitance.

Table 3.2. Values of Parameters Used in Three Antenna Designs

Design Parameters	Antenna 1	Antenna 2	Antenna 3
Substrate Length (L_s)	32 mm	44.44 mm	46 mm
Substrate Width (W_s)	33.5 mm	44.44 mm	46 mm
Effective Ground Length (L_g - G_p)	10.44 mm	14.24 mm	9 mm
Ground Width (W_g)	24.44 mm	33.33 mm	39 mm
Hexagonal patch Circumradius (R)	12 mm	15 mm	17.5 mm
Ground Reduction factor (G_p)	14 mm	19 mm	28 mm
Feed point radius from O (f_r)	10 mm	14 mm	17.5 mm
Slot radius (r_{cut})	0 mm	2.5 mm	3 mm

With an objective to establish $|S_{11}| < -10$ dB, a ground is optimized by reducing the ground by factor G_p. Antenna 1 to Antenna 3 radiates at 7, 5.5 and 5 GHz respectively. To understand the effect of reduced ground on impedance, reflection coefficient for all the three antenna configurations are simulated for three different values of factor G_p i.e for full ground ($G_p = 0$ mm), half ground ($G_p = L_g/2$) and optimized ground. When a reduced ground with G_p = 14, 19 and 28 mm is used with Antenna 1-3, the objective of $|S_{11}| < -10$ dB at 7, 5.5 and 5 GHz, is accomplished as reflected in Figure 3.24, 3.25 and 3.26 respectively. It is observed

that antenna with reduced ground can improve reflection coefficient at a desired frequency. It is important to note that the reduction in area of ground plane is significant while matching the impedance and achieving $|S_{11}| < -10$ dB. In case of antenna 1 and antenna 2 has the optimized G_p at 57.3 % of area reduction but resulting in spurious frequency with the desired frequency as may be observed in Figure 3.24 and Figure 3.25. When the ground is reduced by 77 % the perfect impedance matching is observed in case of antenna 3 as shown in Figure 3.26. The impedance at vertex is very high which is not suitable when probe is placed at vertex as may be observed in Figure 3.24, 3.25 and 3.26 in all the three configurations with full ground i.e. $G_p = 0$ mm. Due to truncation of ground plane, the effective capacitance of the patch compensate the impedance mismatch due to probe feeding at resonant frequency. Probe feeding increases value of impedance but optimum or reduced ground can compensate increase in impedance due to probe location. The phenomenon of impedance matching is further verified with the measurement results. It is interesting to note that reduction in G_p excites modes at lower frequencies.

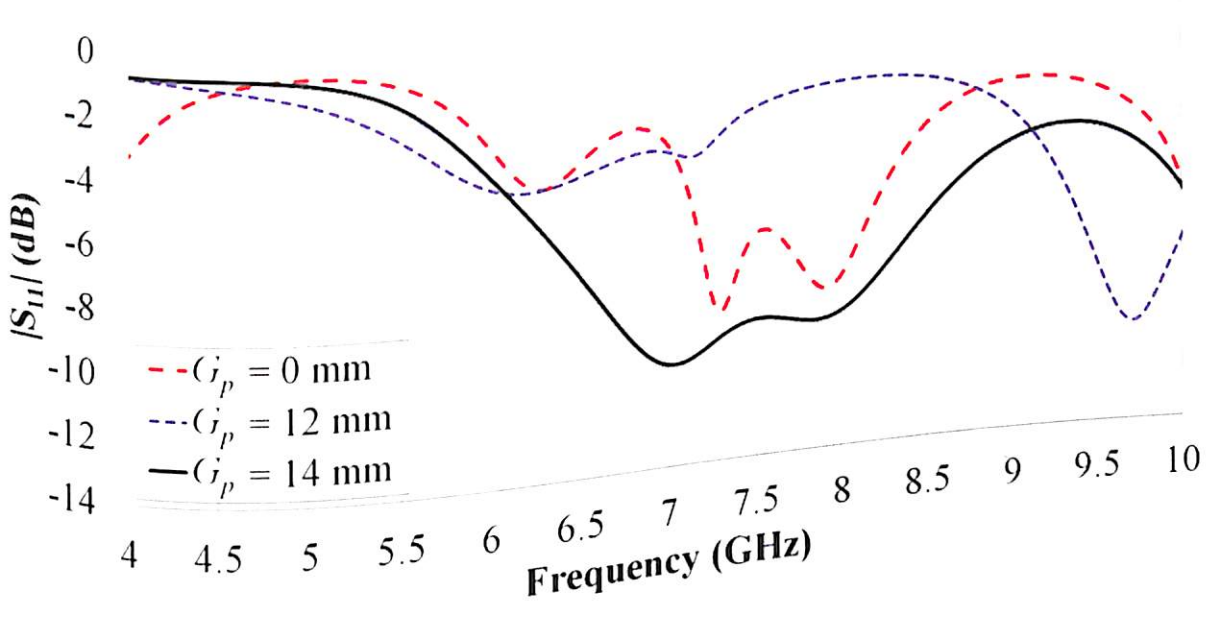

Figure 3.24. Antenna 1 Reflection coefficient, S_{11} (dB)

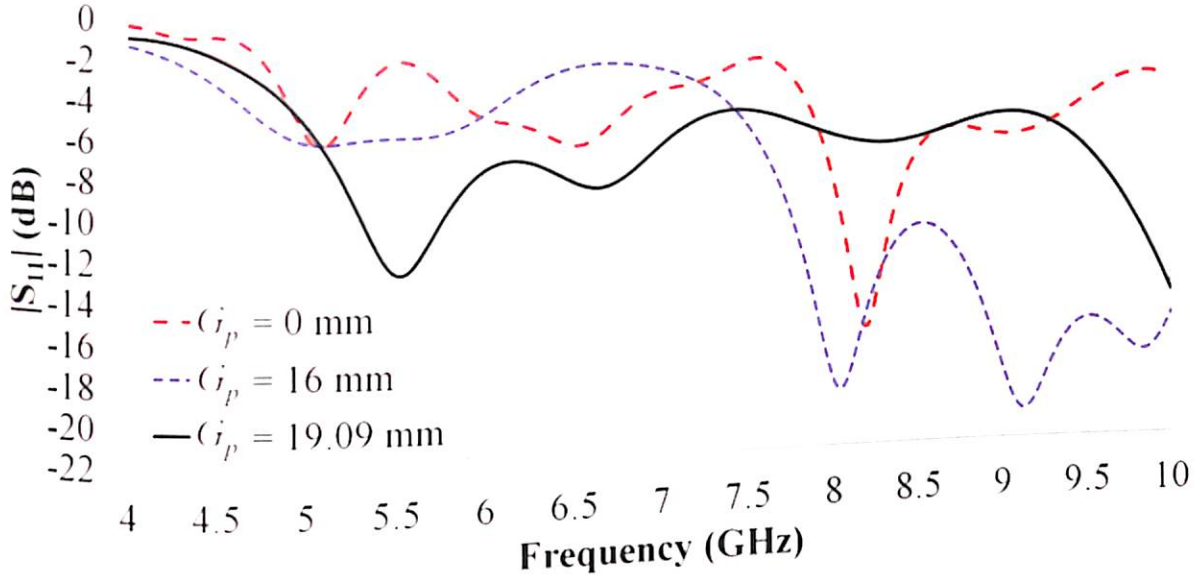

Figure 3.25. Antenna 2 Reflection coefficient, S_{11} (dB)

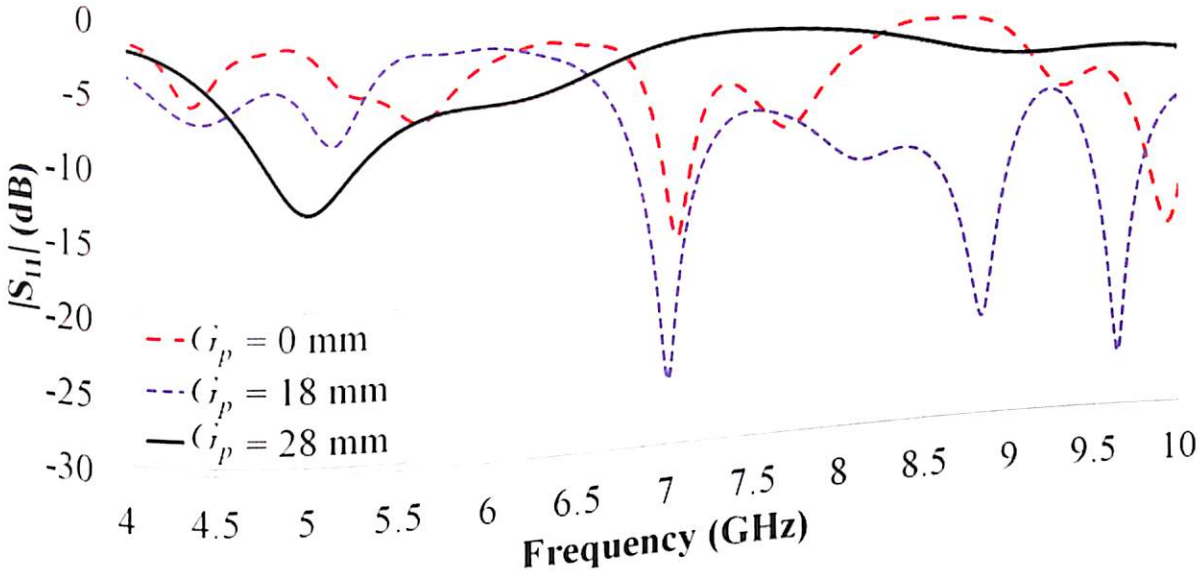

Figure 3.26. Antenna 3 Reflection coefficient, S_{11} (dB)

In order to distinguish the modes at resonating frequencies the modal characteristics at of the antennas are also observed using the magnetic mode field ($\vec{H}$-field) at different phases of the excitation signal at the resonating frequencies. The magnetic mode field ($\vec{H}$-field) for Antenna 1 is displayed in Figure 3.27(a) and 3.27(b) at frequencies 7.02 GHz and 7.86 GHz respectively. The magnetic mode field ($\vec{H}$-field) for Antenna 2 is reflected in Figure 3.27(c) and 3.27(d) at frequencies 5.5 GHz and 6.64 GHz respectively.

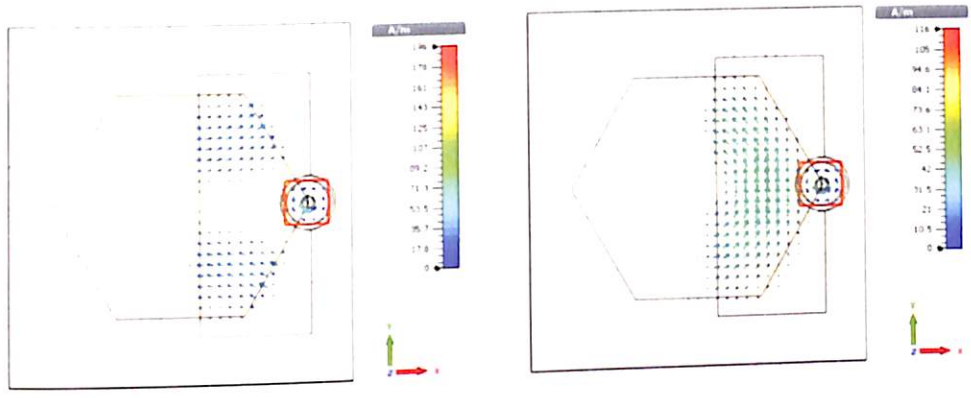

(a) Antenna 1 at 7.02 GHz at 90° phase (b) Antenna 1 at 7.86 GHz at 90° phase

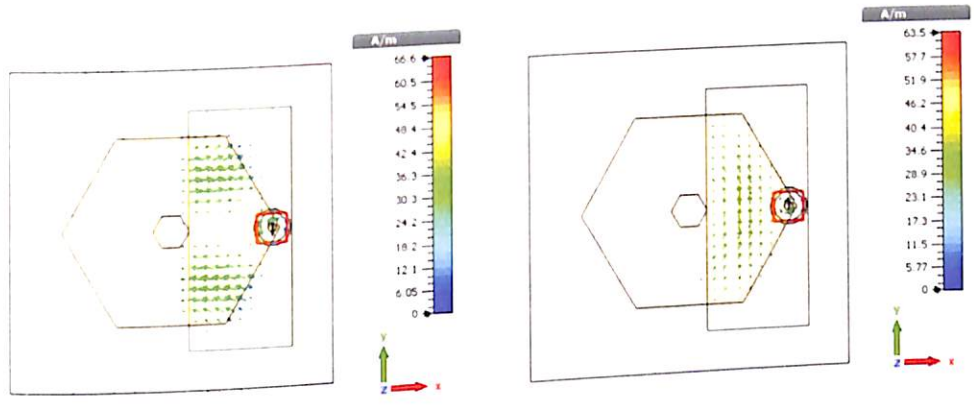

(c) Antenna 2 at 5.5 GHz at 90° phase (d) Antenna 2 at 6.64 GHz at 90° phase

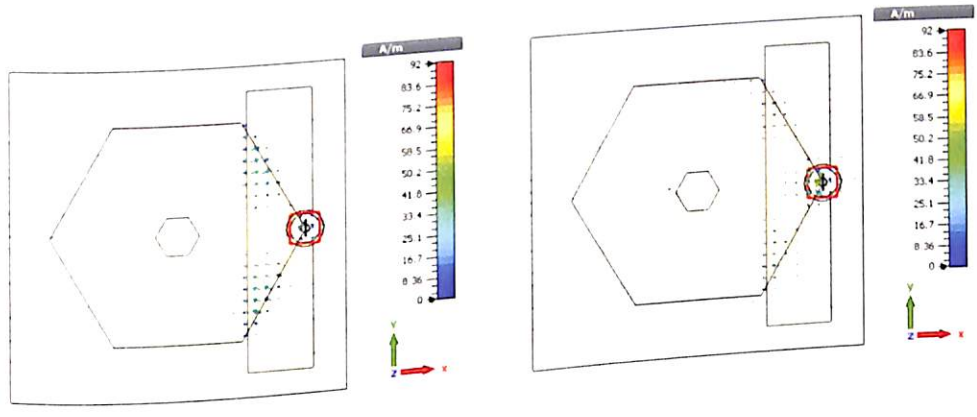

(e) Antenna 3 at 5 GHz at 45° phase (f) Antenna 3 at 5 GHz at 90° phase

Figure 3.27. Magnetic mode field of the antennas.

The magnetic mode field ($\vec{H}$-field) for Antenna 3 is reflected in Figure 3.27(e) and 3.27(f) at frequencies 5 GHz at phases at 45° and 90° respectively. The magnetic mode field analysis suggests that frequencies 7.02, 5.5 and 5 GHz correspond to same mode while frequencies

7.86 and 6.64 GHz have same mode. Since the second mode is suppressed in antenna 39 the two different modes are plotted at phases 45° and 90°.

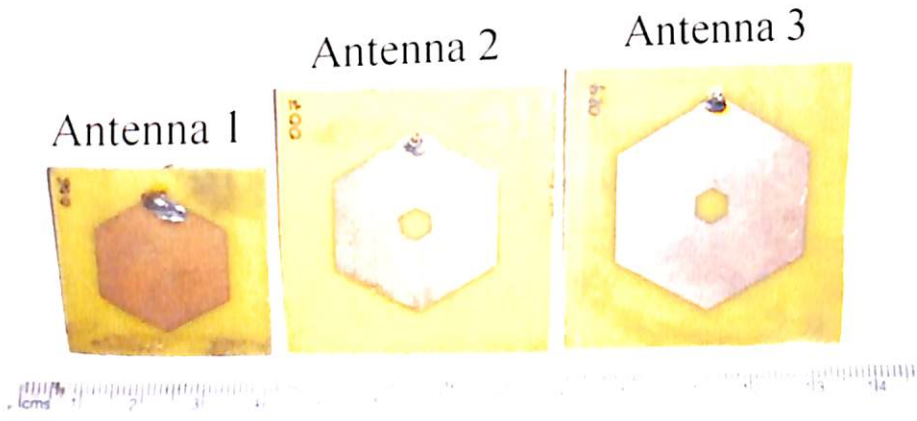

(a)

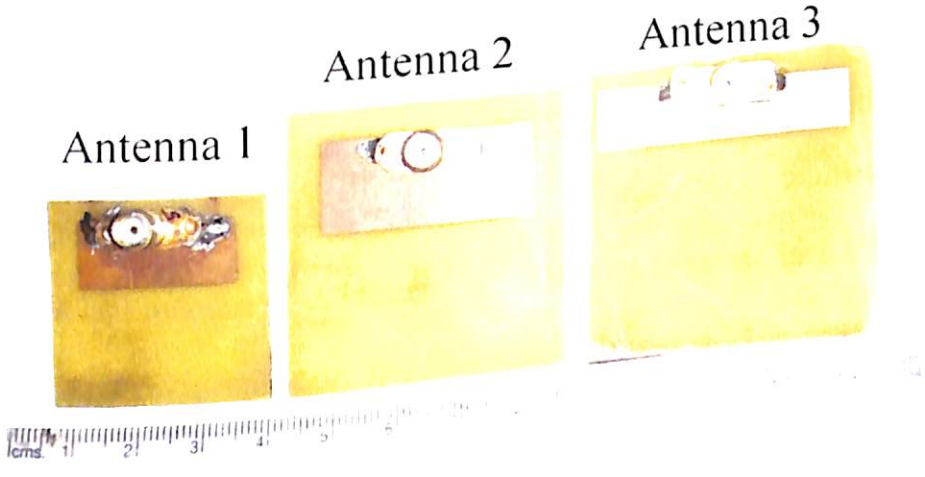

(b)

Figure 3.28. Antenna 1- 3 prototypes (a) Front (b) Back.

The picture of all antenna prototypes, as designed and, are shown in Figure 3.28. To characterize the fabricated antennas for return loss and impedance, a vector network analyzer (VNA) (Keysight N9928A) is used. The return loss of the fabricated antennas is measured and is shown in Figure 3.29.

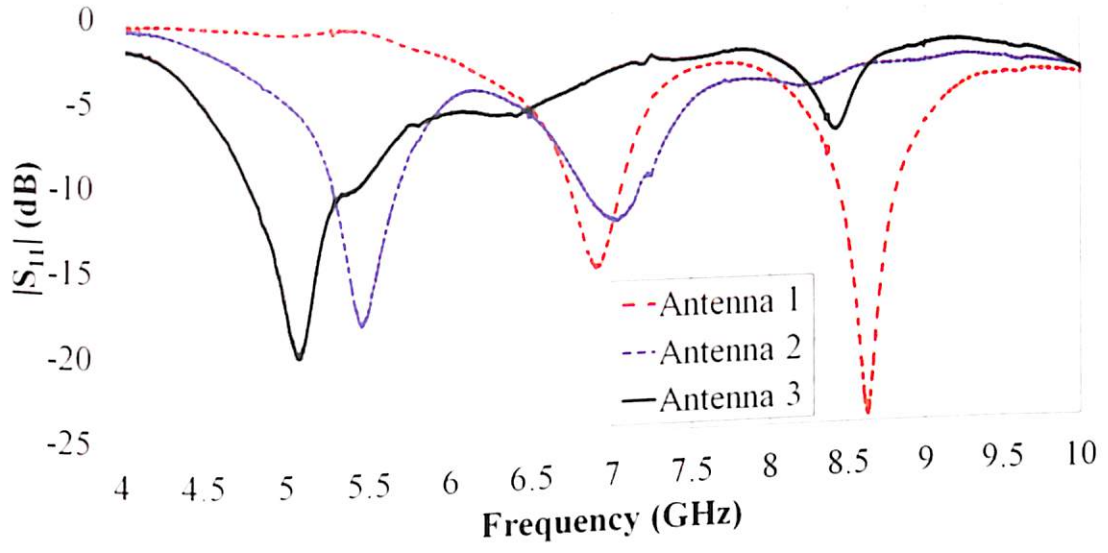

Figure 3.29. Measured Return loss, $|S_{11}|$ (in dB)

The antenna 1, antenna 2 and antenna 3 resonate at 7, 5.5 and 5 GHz respectively. It can be observed from Figure 3.29 that the frequency shifts from 7 to 5.5 GHz, when antenna 1 and antenna 2 return loss are compared due change in dimensions but antenna behavior remains unchanged. Vertex-fed hexagonal patch antenna generates multi-mode response in case of antenna 2 and antenna 3. Additional resonances can create interference in diversity applications thus spurious radiation needs to be suppressed. The presence of spurious radiation at 7 GHz is also observed in case of antenna 2. Similarly, spurious frequency is also observed in return loss of antenna 1 at 8.8 GHz in X-band as shown in Figure 3.29. Further reduction of ground plane evidently suppresses spurious frequency but with the slight shift of resonating frequency from 5.5 to 5 GHz, due change in the radius the hexagon from 15 to 17.5 mm. An undesired mode can be suppressed by reduced ground technique where monopole radiation characteristics are not an issue. It is interesting to note that there is a 200 MHz enhancement in the impedance bandwidth when antenna 2 and antenna 3 is compared. As the ground plane reduces, the antenna capacitance reduces, which in turn compensates the inductive probe. Based on the observations of measured return loss, it can be concluded that ground plane dimensions play significant role in matching the impedance of the probe.

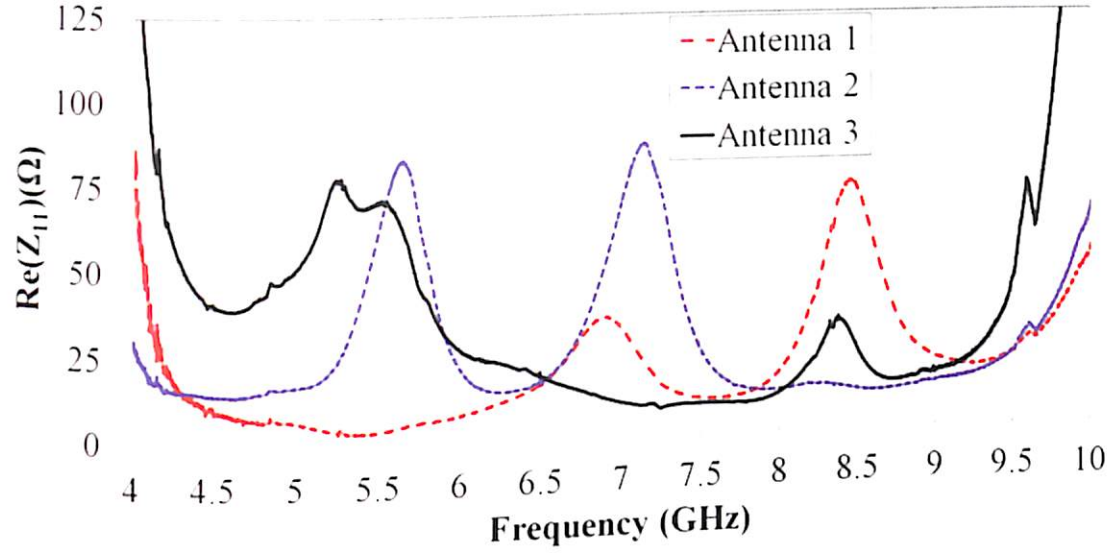

(a)

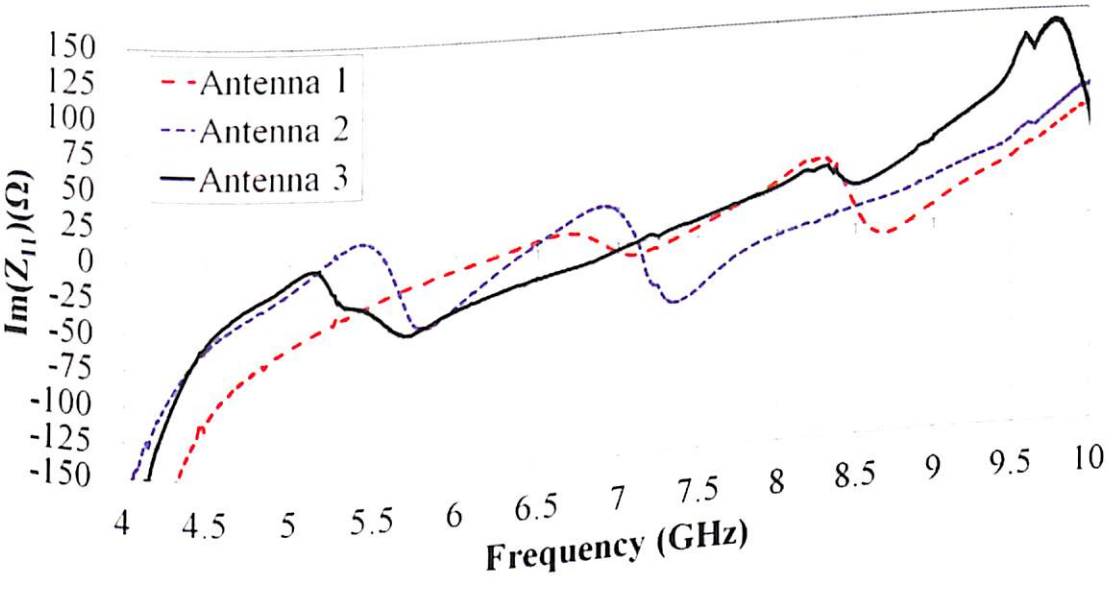

(b)

Figure 3.30. Variation of the input impedance of the proposed antennas (a) Real part (b) Imaginary part.

The value of the impedance Z_{11} is $33 + j\ 0.55$ at 7 GHz, $53.92 + j\ 18.94\ \Omega$ at 5.5 GHz and $53.37 - j\ 5.2\ \Omega$ at 5 GHz for Antenna 1- 3 respectively is shown in Figure 3.30. By observing the measured value of impedances for three different antenna configurations, it suggests that the inductive input impedance of the hexagonal patch is tuned by ground plane reduction

factor, G_p (see Figure 3.30). Although ideally reactive impedance should be zero, small value of reactance is observed. One of the reasons for difference from the ideal value is fabrication tolerance. Real value of impedance is close to expected value of 50 Ω i.e. impedance of the probe, in case of Antenna 3.

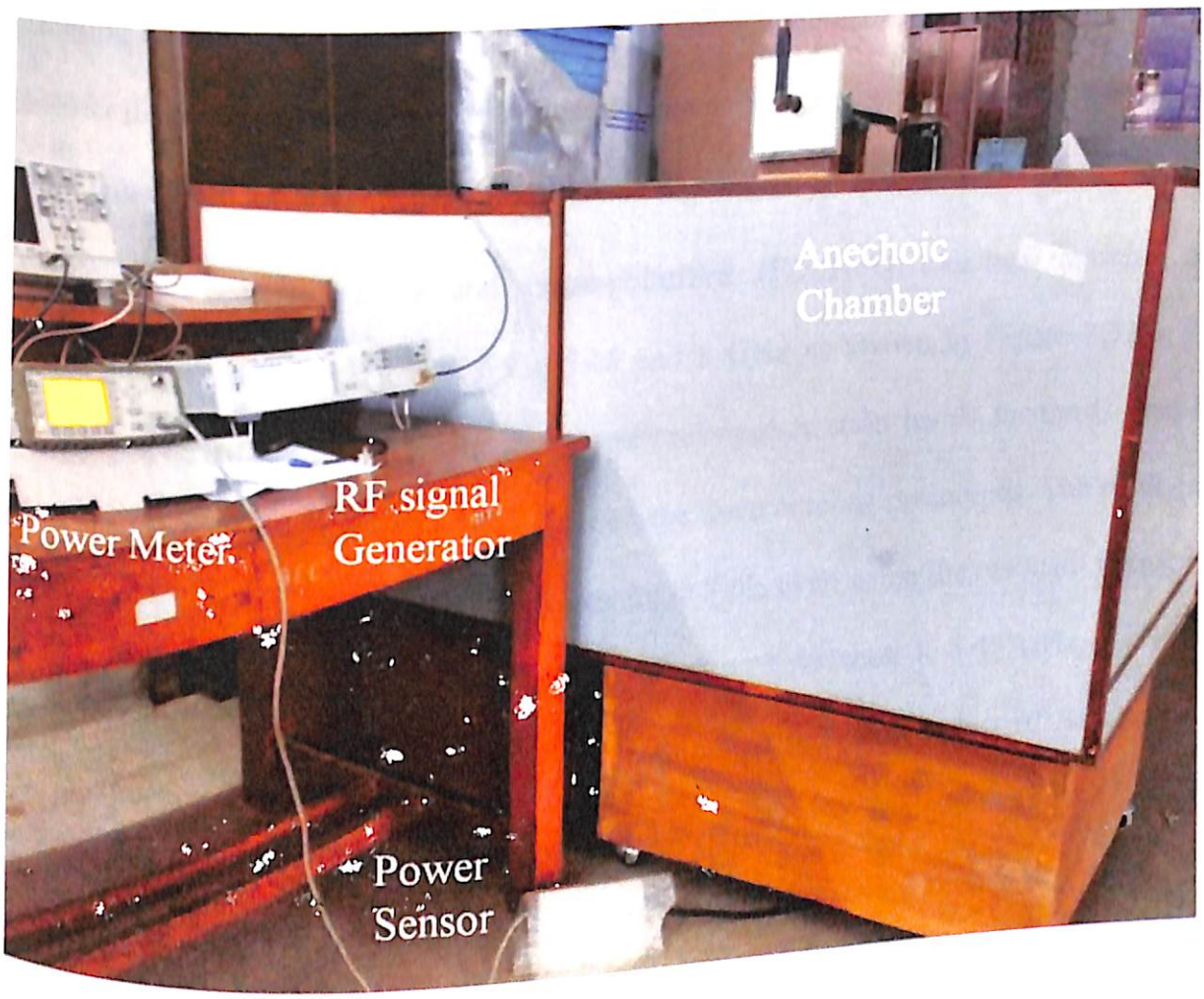

Figure 3.31. Experimental measurement setup [BITS-Pilani].

The radiation pattern measurements of developed antenna prototypes are measured in an anechoic environment at their resonant frequencies using the measurement setup as shown in Figure 3.31. Pre-calibrated standard Dual Ridge Horn (DRH) is used as a transmitter to measure the absolute farfield gain of the fabricated antennas for the two fundamental planes is obtained. For the measurement of farfield gain, a CW Power Sensor (Agilent E-4412A) and a Power Meter (Agilent E-4418B) are used to sense and measure the received power while RF Signal Generator (Keysight N5173B) is used transmit power through the

transmitting (DRH) antenna. The DRH antenna provides gain of 8.5 dB and 6 dB in the two different planes which are further used to calculate the antenna gain. The antenna under test is rotated from 0 to 350 in 10 increments while losses due to cable, the path loss and the absolute transmitted and received power are also measured to calculate antenna gain. The transmitting antenna is 60 cm apart from the receiving antenna which is greater than the Fraunhofer distance required. RF Signal Generator generates a power of 18 dBm. Finally, the received power is measured and data are used to calculate the farfield gain.

The co-polarized (Eco/Hco) and cross-polarized (Ecx/Hcx) radiation patterns are measured for the Antenna 1 - 3 at 6.91, 5.45 and 5 GHz as shown in Figure 3.32(a - c) respectively. The difference between the co-and cross-polarization levels for the E- and H-plane at antenna bore-sight is around 20 dB in all the three antenna prototypes. The peak gain at the antenna bore-sight is approximately constant at 3 dB even when the resonant frequency shifts from higher to lower band i.e. 6.91 GHz in case of Antenna 1, 5.45 GHz in case of Antenna 2 and 5.01 GHz in case of Antenna 3. Although the patch radius of Antenna 3 is 1.45 times the Antenna 1 but the gain of Antenna 3 is approximately equal to gain of Antenna 1 at lower frequency due to the fact that the bandwidth of Antenna 3 higher as compared to Antenna 1 which appears to follow Bode-Fano criterion which states wider bandwidth can be achieved at an expense of higher reflection coefficient (Pozar 2012).

The null of the cross polarization level are centred at 0° for all the three antenna prototypes. Due to the reduced ground plane, the proposed antennas have quasi-monopole radiation patterns. The gain of proposed Antenna 3 is calculated using Friss transmission equation and data collected from radiation pattern measurement is found to be 3 dB. The 3-dB beamwidth are approximately 60° and 50° for the E- and H-plane respectively. The proposed Antenna 3 can be utilized for WLAN (UNII-1) applications.

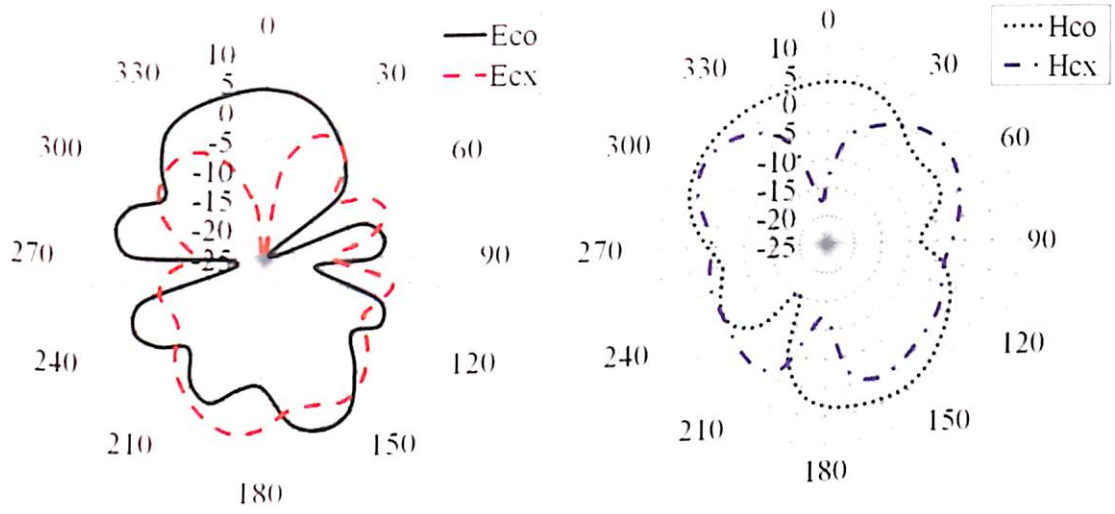

(a) Antenna 1 at 6.91 GHz

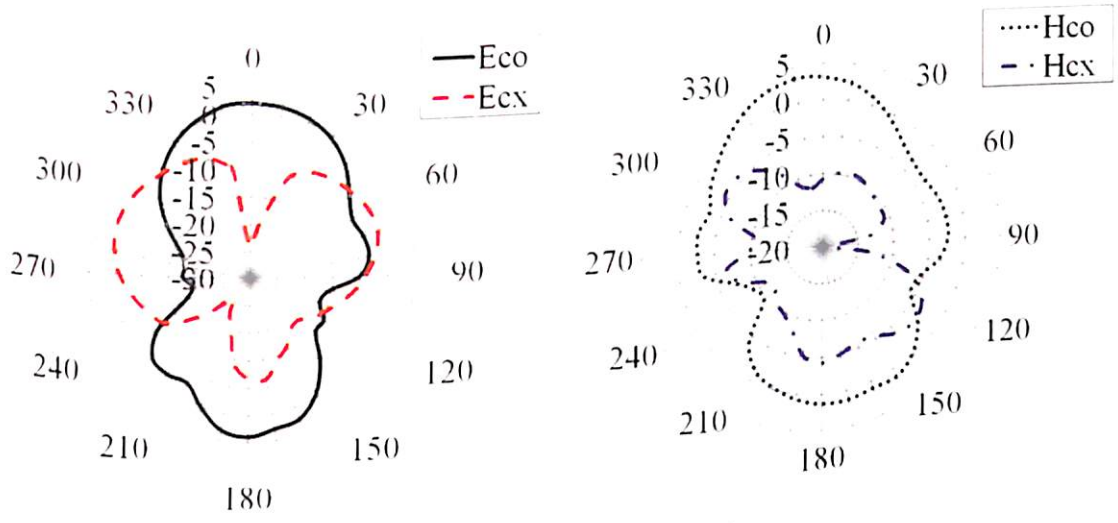

(b) Antenna 2 at 5.45 GHz

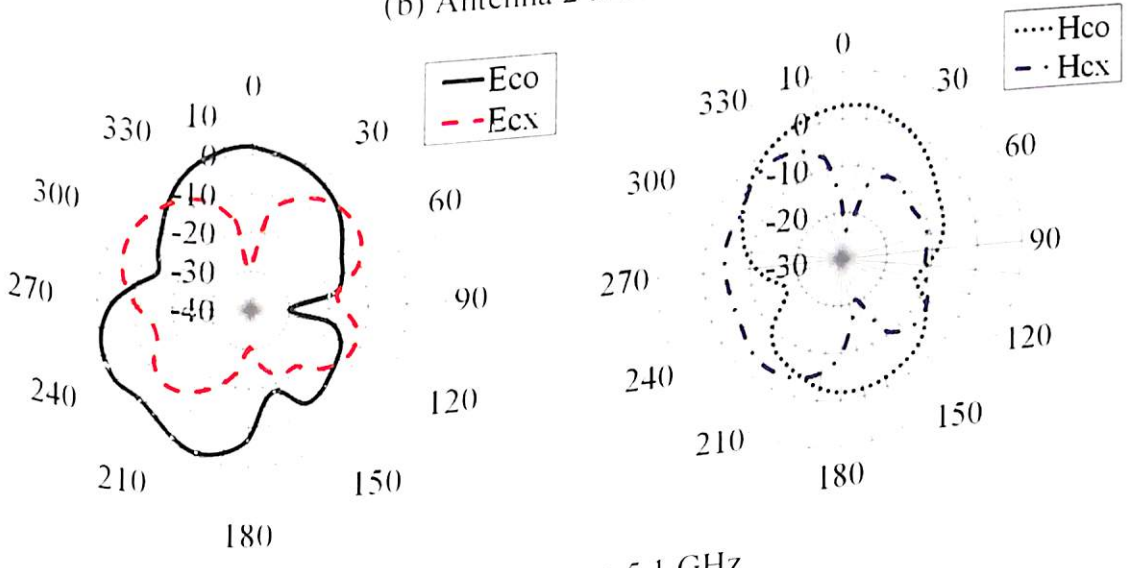

(c) Antenna 3 at 5.1 GHz

Figure 3.32. Measured Co- and Cross-polar patterns.

3.6. Conclusion

The aim of this chapter has been accomplished by investigation of reduced ground technique for spurious radiation suppression in probe fed hexagonal antenna. In this chapter, effect of hexagonal slot and ground reduction in a probe-fed hexagonal patch antenna design is studied and analyzed. One more resonant frequency near 7 GHz is observed but equivalent circuit modeling suggests that the additional frequency is due to probe-to-patch junction capacitance. Desired frequency is excited when the length of ground plane of vertex-fed hexagonal C-Band antenna is reduced from 37 mm to 9 mm. As a result, impedance matching at 5 GHz and frequency suppression at 7 GHz is observed. The proposed compact C-Band antenna has a bandwidth of 600 MHz and a gain of 3.84 dB around 5 GHz, out of which 67% can be used for indoor WLAN (UNII-1) applications.

Due to ground reduction, it is observed that the impedance bandwidth (340 MHz) of the hexagonal patch antenna is narrowed by the introduction of inductance due to direct probe feeding. The maximum gain achieved by proposed antenna at frequency 8.35 GHz is found to be 2.91dB (main lobe magnitude). Finally, it can be concluded from the chapter the ground plane reduction is simple and straightforward which can suppress spurious radiation, match impedance for desired frequency or excite lower mode and can improve cross polarization levels. The lowest or fundamental mode excitation of probe fed hexagonal antenna when fed at the vertex will be illustrated in the next chapter of the thesis.